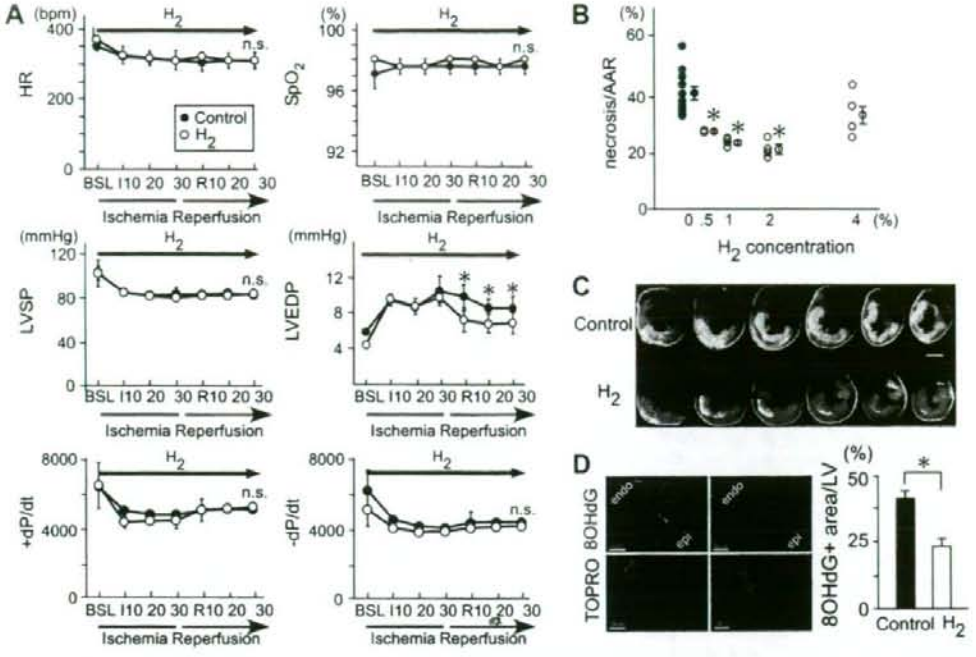

Fig. 3. Inhalation of H_2 reduces infarct size induced by ischemia–reperfusion injury. (A) Changes in heat rate (HR), oxygen saturation by pulse oximetry (SpO_2), and LV systolic pressure (LVSP), LV diastolic pressure (LVEDP) and LV peak positive and negative d*P*/d*t* were monitored during ischemia–reperfusion injury ($n = 5$ in each group). (B) H_2-dependent decrease in infarct size is expressed as the ratio of total infarct area/AAR ($^*P < 0.05$, compared to control group). (C) Representative photographs of serial heart sections obtained from rats subjected to myocardial ischemia–reperfusion injury in the presence or absence of H_2 inhalation. Bar = 2 mm. (D) Immunohistochemical staining with antibodies against 8-OHdG was performed 24 h after ischemia–reperfusion injury. Quantification of 8-OHdG immunoreactive area was expressed as percentage of total LV area at serial short axis sections ($n = 5$, $^*P < 0.05$, H_2 inhalation group compared to control group). endo, endocardium; epi, epicardium.

pressure, LV peak positive and negative LV d*P*/d*t*, between the control group and the 2% H_2 gas inhalation group. Notably, LV-end-diastolic pressure after reperfusion was significantly lower in H_2 gas inhalation group compared to control group ($n = 5$, $^*P < 0.05$).

In the absence of H_2 gas inhalation, infarct size following ischemia–reperfusion was 41.6 ± 2.5% of the area at risk ($n = 9$). By comparison, inhalation of 0.5–2% H_2 gas significantly reduced infarct size, with 2% H_2 gas providing the most prominent effects (21.2 ± 1.6% of area at risk, $n = 4$, Fig. 3B and C). There was no significant difference in area at risk/LV among control group and H_2 gas inhalation groups (data not shown). Consistent with those observations, the quantitative determination of 8-hydroxydeoxyguanosine (8-OHdG) immunoreactive area, a biomarker of oxidative stress, revealed that the level of oxidative injury elicited in the 'at risk' area was significantly smaller in the group receiving 2% H_2 gas inhalation than that of control group ($n = 5$, $^*P < 0.05$, Fig. 3D).

Inhalation of H_2 gas reduces LV remodeling after ischemia–reperfusion injury

To determine the impact of H_2 inhalation at the time of ischemia–reperfusion on pathological LV remodeling, LV morphology and function were monitored by echocardiography 30 days after myocardial ischemia–reperfusion injury. Control rats showed maladaptive pathological remodeling after myocardial infarction, including dilatation of LV cavity, reduced LV systolic function. Notably, inhalation of H_2 gas during myocardial ischemia–reperfusion reduced pathological remodeling after myocardial infarction (Fig. 4).

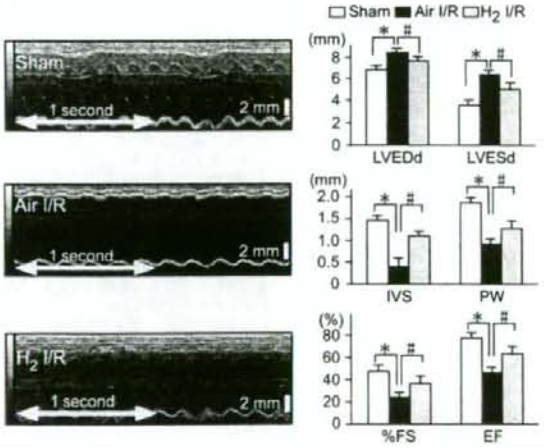

Fig. 4. Inhalation of H_2 gas reduces adverse LV remodeling. Representative M-mode echocardiographic images of sham-operated (sham), ischemia–reperfusion with air inhalation (Air_I/R), and ischemia–reperfusion with H_2 inhalation (H_2_I/R). Measurement of M-mode echocardiographic images in each group. LVEDd, LV endodiastolic diameter (μm); LVESd, LV endosystolic diameter (μm); IVC, intraventricular septum diameter (μm); PW, posterior wall thickness (μm); FS, fractional shortening (%); EF, ejection fraction (%) ($n = 5$, $^*P < 0.05$, compared to sham-operated group; $^\#P < 0.05$, compared to Air_I/R group).

Discussion

This is the first study to demonstrate that inhalation of H_2 gas, at an incombustible level, limit the extent of myocardial infarction

resulting from myocardial ischemia–reperfusion injury, and thereby preserve LV function *in vivo*. The cardioprotective effect of H_2 gas was also confirmed *ex vivo* Langendorff-perfused hearts subjected to anoxia-reoxygenation injury. The anti-oxidant properties of H_2 were confirmed by the demonstration that (1) H_2 improves the recovery of LV function during reoxygenation after anoxia, one of the oxidative stress model, in isolated perfused hearts; (2) inhalation of H_2 gas ameliorates the level of 8-OHdG immunoreactivity in the 'at risk' area for infarction. The anti-oxidant action of molecular H_2 may be explained, at least partially, by direct ROS scavenging effect. However, it remains unclear if the anti-oxidant action of H_2 is also ascribed to the activation of the reperfusion injury salvage kinase pathways or a direct effect on mitochondrial energetics.

Gas inhalation as disease therapy has received recent interest. There are three endogenous gas signaling molecules, known as gasotransmitters, include nitric oxide (NO), carbon monoxide (CO), and hydrogen sulfate (H_2S). The increased production of these gases under stress conditions may reflect the active involvement of these gases in the protective response. In pre-clinical experimental models of disease, including ischemia–reperfusion injury, the inhalation of exogenous CO or H_2S has produced a favorable outcome for most vital organs [19–22]. However, the inherent toxicity of these gases must be investigated for gas inhalation to be considered an effective therapeutic strategy. It is unknown if the therapeutically effective threshold for CO or H_2S can be attained locally in target organs without delivering a potentially toxic level of the gasses via the lungs.

H_2 is not produced endogenously in mammalian cells since the hydrogenase activity responsible for the formation of H_2 gas has not been identified [23]. The spontaneous production of H_2 gas in the human body occurs via fermentation of undigested carbohydrates by resident enterobacterial flora. H_2 is transferred to the portal circulation and excreted through the breath in significant amounts. We demonstrated that inhaled H_2 at therapeutic dose has no adverse effects on the saturation level of arterial oxygen (SpO_2) or hemodynamic parameters, including heart rate and LV pressure. H_2 dissolved in the blood is distributed to tissues proportional to regional blood flow, and is rapidly eliminated by the lungs. Accordingly, the H_2 gas clearance method was employed to measure local blood flow in various tissues [24]. Since the heart is one of the most highly perfused tissues, the intramyocardial H_2 concentration increases immediately following inhalation of H_2, and attaining to almost compatible levels of that observed in arterial blood within 10 min. Of note, the regional H_2 concentration in the ischemic myocardium reaches at two thirds of the value observed in the non-ischemic myocardium. This may occur through gaseous diffusion from the blood in the ventricular cavity and/or adjacent non-ischemic myocardium. These findings indicate that administration of H_2 gas by inhalation, in patients with totally coronary artery occlusion, can efficiently increase the regional concentration of H_2 in the 'at risk' area for myocardial infarction before reestablishing coronary blood flow within the occluded infarct-related artery.

We demonstrated that inhalation of H_2 gas is promising strategies to alleviate ischemia–reperfusion injury at the time of recanalization of coronary artery. When translated into the clinical practice, inhalation of H_2 gas must be most frequently applied in the treatment of patients with acute myocardial infarction in conjunction with routinely performed PCI procedures. Further understanding of the mechanisms underlying the signaling pathways involved in H_2-mediated anti-oxidant activity, and the capacity of H_2 to influence cellular metabolism, is required to fully exploit inhalation of H_2 gas as a therapeutic strategy.

Acknowledgments

We thank M. Okada (NIHON KODEN), S. Kotouda (LMS laboratory and Medical Supplies), C. Ogawa, K. Nishimaki, M. Kamimura, M. Abe, Y. Miyake, H. Kawaguchi, H. Shiozawa, and M. Ono for their technical assistance. M. Sano is a core member of the Global Center-of-Excellence (GCOE) for Human Metabolomics Systems Biology from MEXT. This work was supported by a PRESTO (Metabolism and Cellular Function) grant from the Japanese Science and Technology Agency awarded to M. Sano.

Appendix A. Supplementary data

Supplementary data associated with this article can be found, in the online version, at doi:10.1016/j.bbrc.2008.05.165.

References

[1] A. Volpi, C. De Vita, M.G. Franzosi, E. Geraci, A.P. Maggioni, F. Mauri, E. Negri, E. Santoro, L. Tavazzi, G. Tognoni, Determinants of 6-month mortality in survivors of myocardial infarction after thrombolysis. Results of the GISSI-2 data base. The Ad hoc Working Group of the Gruppo Italiano per lo Studio della Sopravvivenza nell'Infarto Miocardico (GISSI)-2 Data Base, Circulation 88 (1993) 416–429.
[2] E.C. Keeley, J.A. Boura, C.L. Grines, Primary angioplasty versus intravenous thrombolytic therapy for acute myocardial infarction: a quantitative review of 23 randomised trials, Lancet 361 (2003) 13–20.
[3] E. Braunwald, R.A. Kloner, Myocardial reperfusion: a double-edged sword?, J Clin. Invest. 76 (1985) 1713–1719.
[4] D.M. Yellon, D.J. Hausenloy, Myocardial reperfusion injury, N. Engl. J. Med. 357 (2007) 1121–1135.
[5] J.L. Zweier, Measurement of superoxide-derived free radicals in the reperfused heart. Evidence for a free radical mechanism of reperfusion injury, J. Biol. Chem. 263 (1988) 1353–1357.
[6] R. Bolli, B.S. Patel, M.O. Jeroudi, E.K. Lai, P.B. McCay, Demonstration of free radical generation in "stunned" myocardium of intact dogs with the use of the spin trap alpha-phenyl *N*-*tert*-butyl nitrone, J. Clin. Invest. 82 (1988) 476–485.
[7] T. Vanden Hoek, L.B. Becker, Z.H. Shao, C.Q. Li, P.T. Schumacker, Preconditioning in cardiomyocytes protects by attenuating oxidant stress at reperfusion, Circ. Res. 86 (2000) 541–548.
[8] J.T. Flaherty, B. Pitt, J.W. Gruber, R.R. Heuser, D.A. Rothbaum, L.R. Burwell, B.S. George, D.J. Kereiakes, D. Deitchman, N. Gustafson, et al., Recombinant human superoxide dismutase (h-SOD) fails to improve recovery of ventricular function in patients undergoing coronary angioplasty for acute myocardial infarction, Circulation 89 (1994) 1982–1991.
[9] V.J. Richard, C.E. Murry, R.B. Jennings, K.A. Reimer, Therapy to reduce free radicals during early reperfusion does not limit the size of myocardial infarcts caused by 90 minutes of ischemia in dogs, Circulation 78 (1988) 473–480.
[10] C. Penna, R. Rastaldo, D. Mancardi, S. Raimondo, S. Cappello, D. Gattullo, G. Losano, P. Pagliaro, Post-conditioning induced cardioprotection requires signaling through a redox-sensitive mechanism, mitochondrial ATP-sensitive K^+ channel and protein kinase C activation, Basic Res. Cardiol. 101 (2006) 180–189.
[11] J.M. Downey, M.V. Cohen, A really radical observation—a comment on Penna et al., Basic Res. Cardiol. 101 (2006) 190–191.
[12] I. Ohsawa, M. Ishikawa, K. Takahashi, M. Watanabe, K. Nishimaki, K. Yamagata, K. Katsura, Y. Katayama, S. Asoh, S. Ohta, Hydrogen acts as a therapeutic antioxidant by selectively reducing cytotoxic oxygen radicals, Nat. Med. 13 (2007) 688–694.
[13] K. Fukuda, S. Asoh, M. Ishikawa, Y. Yamamoto, I. Ohsawa, S. Ohta, Inhalation of hydrogen gas suppresses hepatic injury caused by ischemia/reperfusion through reducing oxidative stress, Biochem. Biophys. Res. Commun. 361 (2007) 670–674.
[14] M. Tani, Y. Suganuma, H. Hasegawa, K. Shinmura, Y. Hayashi, X. Guo, Y. Nakamura, Changes in ischemic tolerance and effects of ischemic preconditioning in middle-aged rat hearts, Circulation 95 (1997) 2559–2566.
[15] K. Shinmura, K. Tamaki, R. Bolli, Short-term caloric restriction improves ischemic tolerance independent of opening of ATP-sensitive K^+ channels in both young and aged hearts, J. Mol. Cell. Cardiol. 39 (2005) 285–296.
[16] K. Shinmura, K. Tamaki, K. Saito, Y. Nakano, T. Tobe, R. Bolli, Cardioprotective effects of short-term caloric restriction are mediated by adiponectin via activation of AMP-activated protein kinase, Circulation 116 (2007) 2809–2817.
[17] J.P. Headrick, Aging impairs functional, metabolic and ionic recovery from ischemia–reperfusion and hypoxia-reoxygenation, J. Mol. Cell. Cardiol. 30 (1998) 1415–1430.
[18] J. Endo, M. Sano, J. Fujita, K. Hayashida, S. Yuasa, N. Aoyama, Y. Takehara, O. Kato, S. Makino, S. Ogawa, K. Fukuda, Bone marrow derived cells are involved in the pathogenesis of cardiac hypertrophy in response to pressure overload, Circulation 116 (2007) 1176–1184.

[19] C. Szabo, Hydrogen sulphide and its therapeutic potential, Nat. Rev. Drug Discov. 6 (2007) 917–935.
[20] J.W. Elrod, J.W. Calvert, J. Morrison, J.E. Doeller, D.W. Kraus, L. Tao, X. Jiao, R. Scalia, L. Kiss, C. Szabo, H. Kimura, C.W. Chow, D.J. Lefer, Hydrogen sulfide attenuates myocardial ischemia–reperfusion injury by preservation of mitochondrial function, Proc. Natl. Acad. Sci. USA 104 (2007) 15560–15565.
[21] R. Foresti, M.G. Bani-Hani, R. Motterlini, Use of carbon monoxide as a therapeutic agent: promises and challenges, Intensive Care Med. (2008).
[22] A. Kobayashi, K. Ishikawa, H. Matsumoto, S. Kimura, Y. Kamiyama, Y. Maruyama, Synergetic antioxidant and vasodilatory action of carbon monoxide in angiotensin II-induced cardiac hypertrophy, Hypertension 50 (2007) 1040–1048.
[23] M.W. Adams, L.E. Mortenson, J.S. Chen, Hydrogenase, Biochim. Biophys. Acta 594 (1980) 105–176.
[24] K. Aukland, B.F. Bower, R.W. Berliner, Measurement of local blood flow with hydrogen gas, Circ. Res. 14 (1964) 164–187.

Biochemical and Biophysical Research Communications 371 (2008) 44–49

Contents lists available at ScienceDirect

Biochemical and Biophysical Research Communications

journal homepage: www.elsevier.com/locate/ybbrc

Role of the hinge region of glucocorticoid receptor for HEXIM1-mediated transcriptional repression

Noritada Yoshikawa [a,b,1], Noriaki Shimizu [a,1], Motoaki Sano [c], Kei Ohnuma [a,b], Satoshi Iwata [a], Osamu Hosono [a,b], Keiichi Fukuda [c], Chikao Morimoto [a,b], Hirotoshi Tanaka [a,b,*]

[a] Division of Clinical Immunology, Advanced Clinical Research Center, Institute of Medical Science, University of Tokyo, 4-6-1, Shirokanedai Minato-ku, Tokyo 108-8639, Japan
[b] Department of Rheumatology and Allergy, Research Hospital, Institute of Medical Science, University of Tokyo, Japan
[c] Department of Regenerative Medicine, Keio University School of Medicine, Tokyo, Japan

ARTICLE INFO

Article history:
Received 10 March 2008
Available online 11 April 2008

Keywords:
Glucocorticoid
Hinge region
Nuclear receptor
HEXIM1
P-TEFb
RNA
Elongation
Transcription

ABSTRACT

We previously reported that HEXIM1 (hexamethylene bisacetamide-inducible protein 1), which suppresses transcription elongation via sequestration of positive transcription elongation factor b (P-TEFb) using 7SK RNA as a scaffold, directly associates with glucocorticoid receptor (GR) to suppress glucocorticoid-inducible gene activation. Here, we revealed that the hinge region of GR is essential for its interaction with HEXIM1, and that oxosteroid receptors including GR show sequence homology in their hinge region and interact with HEXIM1, whereas the other members of nuclear receptors do not. We also showed that HEXIM1 suppresses GR-mediated transcription in two ways: sequestration of P-TEFb by HEXIM1 and direct interaction between GR and HEXIM1. In contrast, peroxisome proliferator-activated receptor γ-dependent gene expression is negatively modulated by HEXIM1 solely via sequestration of P-TEFb. We, therefore, conclude that HEXIM1 may act as a gene-selective transcriptional regulator via direct interaction with certain transcriptional regulators including GR and contribute to fine-tuning of, for example, glucocorticoid-mediated biological responses.

© 2008 Published by Elsevier Inc.

Glucocorticoid hormone is essential for maintenance of homeostasis and its actions are believed to exclusively be mediated via binding to its cognate receptor glucocorticoid receptor (GR) [1]. The GR is a ligand-dependent transcription factor belonging to the nuclear receptor superfamily. In particular, the GR, mineralocorticoid receptor (MR), androgen receptor (AR), and progesterone receptor (PR), sharing a common structure, compose subfamily NR3C, and are also called oxosteroid receptors because their cognate ligands have C3-ketone group in the steroid A-ring [2]. GR-mediated transcriptional regulation is originally proposed to be mediated via binding of GR to the glucocorticoid response elements (GRE) on the target gene promoters, however, currently considered to be controlled by communication with a variety of cellular factors [3,4]. The GR protein consists of six distinct domains. The N-terminal A/B domains include transactivational function domain 1 (AF-1). The central C-domain constitutes the DNA-binding domain (DBD). The C-terminal E/F-domains contains the ligand-binding domain (LBD) and transactivational function domain 2 (AF-2). The D-domain, which is called hinge region as well, is relatively less conserved across nuclear receptors, and, concerning GR, was initially suggested to be a flexible linker between the DBD and the LBD, allowing proper DNA binding, dimerization, and nuclear translocation of the receptor [5]. Although several reports have raised the possibility that this hinge region mediates the interaction with a certain classes of nuclear proteins [6,7], its precise role in functional regulation of GR remains unknown.

Transcription is a complex process controlled at various steps, such as initiation, elongation, and termination [8]. Recently, it has become evident that the positive transcription elongation factor b (P-TEFb), which is composed of cyclin-dependent kinase 9 (CDK9) and cyclin T1 (CycT1), stimulates transcription elongation via phosphorylating the C-terminal domain of RNA polymerase II [9]. A nuclear protein HEXIM1 (hexamethylene bisacetamide-inducible protein 1) negatively regulates this transcription elongation via sequestration of P-TEFb using 7SK small nuclear RNA as a scaffold [10]. HEXIM1 consists of an N-terminal self-inhibitory domain, a C-terminal inhibitory domain, and a central basic region (BR) conveying nuclear localization signal (NLS) and 7SK-binding domain [10]. On the other hand, a growing body of evidence indicates that HEXIM1 has other functions for modulation of gene expression. For example, HEXIM1 has been shown to directly bind and modulate the activities of transcription factors including ERα [11], GR [12], and CCAAT/enhancer-binding protein α (C/EBPα [13].

* Corresponding author. Address: Division of Clinical Immunology, Advanced Clinical Research Center, Institute of Medical Science, University of Tokyo, 4-6-1, Shirokanedai Minato-ku, Tokyo 108-8639, Japan. Fax: +81 3 5449 5547.
E-mail address: hirotnk@ims.u-tokyo.ac.jp (H. Tanaka).
[1] These authors equally contributed to this work.

0006-291X/$ - see front matter © 2008 Published by Elsevier Inc.
doi:10.1016/j.bbrc.2008.03.155

We previously showed that GR binds to the BR of HEXIM1 to form a separate complex distinct from the HEXIM1/7SK/P-TEFb complex [12]. Moreover, overexpression of HEXIM1 decreases ligand-dependent association between GR and a coactivator transcription intermediate factor-2 (TIF2), resulting in suppression of glucocorticoid-responsive gene activation [12]. Since GR inhibition by HEXIM1 was still preserved even after antisense-mediated knockdown of 7SK, we speculated that HEXIM1 could directly suppress GR-mediated transactivation independent of inhibition of transcription elongation [12]. In the present study, we studied molecular details of this GR-HEXIM1 interaction and revealed that the hinge region of GR is responsible for the interaction with HEXIM1. Moreover, we indicated that HEXIM1 BR differentially modulates two distinct gene regulatory pathways: P-TEFb-dependent transcription elongation and suppression of GR-mediated transactivation via direct binding to the hinge region of the receptor.

Materials and methods

Reagents, antibodies, and cells. Dexamethasone (DEX) and troglitazone (TGZ) were purchased from Sigma. Other reagents were from Nacalai Tesque (Kyoto, Japan) unless otherwise specified. Anti-CDK9 antibody was obtained from Santa Cruz Biotechnology. COS-7 and HeLa cells were obtained from RIKEN Cell Bank (Tsukuba, Japan) and cultured in Dulbecco's modified Eagle's medium (Invitrogen) supplemented with 10% fetal calf serum and antibiotics in a humidified atmosphere at 37 °C with 5% CO_2.

Recombinant DNA. cDNAs of human MR, retinoic acid receptor α (RARα), retinoid X receptor α (RXRα), AR, peroxisome proliferator-activated receptor γ (PPARγ), vitamin D receptor (VDR), and farnesoid X-activated receptor (FXR) were kindly gifted from Drs. R.M. Evans (the Salk Institute, La Jolla, CA), H. Nawata (Kyushu University, Fukuoka, Japan), E.A. Jansson (Karolinska Institutet, Stockholm, Sweden), K. Umesono (Kyoto University, Kyoto, Japan), and D.J. Mangelsdorf (University of Texas, Dallas, TX), respectively. The expression plasmids for human wild-type and various truncated GR and other nuclear receptors were generated by cloning appropriate PCR fragments into pCMX-HA vector as described before [14]. The expression plasmids for the wild-type and BR mutated FLAG-HEXIM1 and glutathione-*S*-transferase (GST)-fused HEXIM1 were generous gifts from Dr. Q. Zhou (UC Berkeley, CA) and described previously [12]. To construct expression plasmids for deletion mutant of the hinge region of GR (488–520 and 491–515a.a.) and PPARγ (173–288a.a.) (pCMX-HA-GRdD1, pCMX-HA-GRdD2, and pCMX-HA-PPARγdD, respectively), cDNAs encompassing the deleted regions with appropriate flanking sequences containing XhoI cloning site were amplified with PCR and subcloned into pCMX-HA-GR and pCMX-HA-PPARγ. To construct the chimeric protein expression plasmids pCMX-HA-GRdD1 + MRD, pCMX-HA-GRdD1 + PPARγD, and pCMX-HA-PPARγdD + GRD, we opened pCMX-HA-GRdD1 and pCMX-HA-PPARγdD at XhoI site, and the cDNA fragments encompassing the hinge region of MR (670–704a.a.), PPARγ (173–288a.a.), and GR (488–520a.a.) were subcloned, respectively. The GRE- and PPAR-response element (PPARRE)-driven reporter plasmids p2xGRE-LUC and p3xPPARRE-LUC, respectively, were described previously [12] and gifted from Dr. E.A. Jansson, respectively.

In vitro protein–protein interaction studies. To obtain the proteins of each nuclear receptor, *in vitro* transcription and translation was performed using various pCMX-HA plasmids as template with the TNT Coupled Reticulocyte Lysate System (Promega) in the presence of [^{35}S] Met (1000 Ci/mmol, Amersham Biosciences). Ten microliters of each protein was added to FLAG-HEXIM1-immobilized FLAG-affinity resin or GST- or GST-HEXIM1-immobilized glutathione Sepharose beads and incubated in binding buffer (25 mM Tris–HCl, pH 7.9, 1 mM DTT, 50 mM NaCl, 1 mM PMSF, and 0.1% (v/v) NP-40) at room temperature for 90 min. Then, the beads were washed, and bound proteins were eluted with 1 M NaCl, analyzed on SDS–polyacrylamide gel electrophoresis (SDS–PAGE), and followed by fluorography.

Sequence alignment. Pretty in SeqWeb package (Genetics Computer Group, Accelrys Inc.) was used with default parameters to align the hinge region sequences of GR to that of the other members of the nuclear receptors.

FLAG-affinity purification. Whole cell extracts were prepared from various FLAG-tagged HEXIM1 expressing HeLa cells, applied to Anti-FLAG M2-agarose beads (Sigma–Aldrich), and incubated for 2 h at room temperature. The beads were washed and bound proteins were eluted with SDS-sample loading buffer, and subjected to Western blot analysis using appropriate antibodies.

Transfection and reporter gene assay. Cells were cultured on 6-cm diameter culture dishes and cell culture medium was replaced with OPTI-MEM medium lacking phenol red (Invitrogen) before transfection. Total amount of the plasmids was kept constant by adding appropriate empty vectors and transfection was performed with TransIT-LT1 (Takara). After 6 h of incubation, media were replaced with fresh OPTI-MEM, and the cells were further cultured with ligands for 24 h at 37 °C. Whole cell extracts were prepared and luciferase enzyme activities were determined using Luciferase Assay System (Promega). Relative light units were normalized to the protein amounts determined with BCA Protein Assay Reagent (PIERCE).

Results

The hinge region of GR was essential for the interaction between GR and HEXIM1

To address the protein–protein interaction of GR with HEXIM1, we investigated which region of GR is essential for the interaction with HEXIM1. We synthesized various [^{35}S] Met-labeled GR mutants *in vitro* (Fig. 1), and applied them onto FLAG-affinity resin bound FLAG-tagged HEXIM1. Since, we preliminarily showed that neither AF-1 nor DBD is prerequisite for the interaction [12], we focused on the relatively C-terminal part of GR including the hinge region and the LBD/AF-2 (D, E, and F domain). As shown in Fig. 1, HEXIM1 bound to not only wild-type GR but also GR 417–777, 487–777, 417–750, 417–640, and 417–520. However, GR 1–489, 1–417, 520–777, and 417–487 did not bind to HEXIM1. These results indicated that the amino acids spanning 487–520, which overlaps with the hinge region, are important for binding to HEXIM1.

Oxosteroid receptors showed amino acid sequence homology in their hinge regions and bound to HEXIM1 in vitro

Among nuclear receptors, amino acid sequence homology of the hinge region was hardly seen except for the oxosteroid receptor subfamily including GR, MR, AR, and PR (Fig. 2A). Given this, we tested whether the representative members of the nuclear receptor superfamily interact with HEXIM1. For that purpose, GST-fused HEXIM1-immobilized beads were incubated with *in vitro* translated nuclear receptors as indicated in Fig. 2B. As expected, HEXIM1 significantly bound to not only GR but also MR and AR, but to neither PPARγ, RARα, RXRα, VDR, nor FXR (Fig. 2B). To further examine the role of the hinge region for the interaction between GR and HEXIM1, we applied domain deletion and swap analyses (Fig. 2C). Deletion of the hinge region (amino acids 488–520 and 491–515) from GR (GRdD1 and GRdD2, respectively) lost the ability of GR to bind to HEXIM1. GRdD1 + MRD, in which the GR hinge

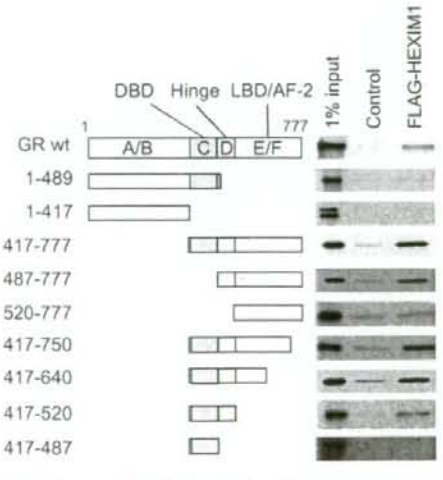

Fig. 1. HEXIM1 interacts with the hinge region of GR. Primary structures of the wild-type and mutant GR are schematically illustrated on the *left*. Numbers depict the positions of amino acids and boxes show the domain structures. FLAG-fused HEXIM1-immobilized beads were incubated with *in vitro* translated [^{35}S]Met-labeled GRs, bound proteins were analyzed on SDS–PAGE followed by fluorography, and representative results are shown.

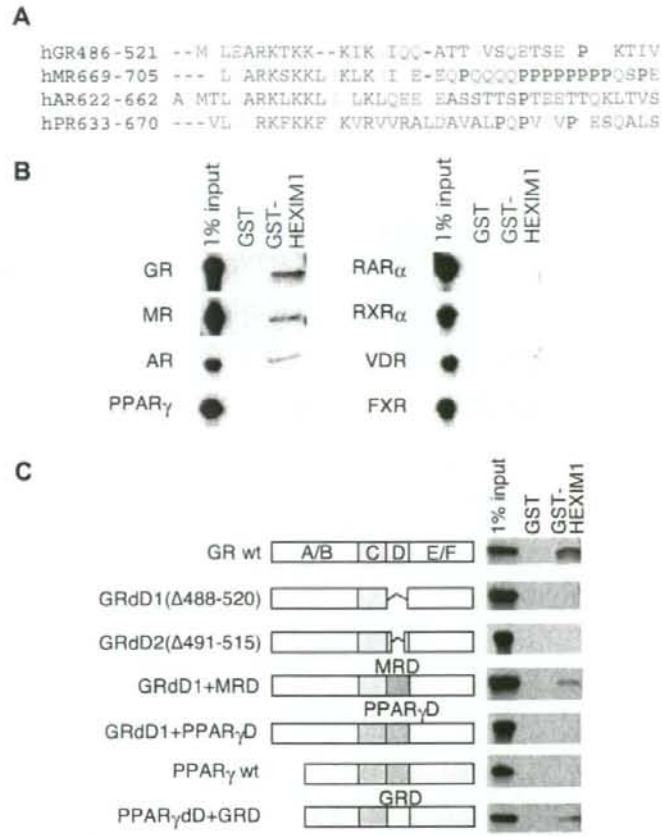

Fig. 2. The structure of the hinge region of the nuclear receptors determines their binding ability to HEXIM1. (A) Pretty in SeqWeb package (Accelrys Inc.) was used with default parameters to align the hinge sequence of GR to those of the all other members of the nuclear receptors. Homology was not significantly detected except for MR, AR, and PR and the multiple alignments of their hinge regions are shown. Dashes represent gaps in the alignment. (B,C) GST or GST-fused HEXIM1-immobilized beads were incubated with *in vitro* translated [^{35}S]Met-labeled proteins as indicated, bound receptors were analyzed on SDS–PAGE followed by fluorography, and representative results are shown. Deletion and swap mutants of the hinge region of GR, MR, and PPARγ are schematically shown on the *left* (C). D, D-domain (hinge region); MRD, PPARγD, and GRD depict the D-domain of MR, PPARγ, and GR, respectively (C).

region was substituted with that of MR, bound to HEXIM1, whereas GRdD1 + PPARγD, in which the GR hinge region was substituted with that of PPARγ, did not. Although wild-type PPARγ did not bind to HEXIM1, PPARγdD + GRD, in which the PPARγ hinge region was substituted with that of GR, acquired the ability to bind to HEXIM1 (Fig. 2C). Collectively, we concluded that HEXIM1 binds particular members of nuclear hormone receptors, especially oxosteroid receptors including GR, and that the hinge regions of those receptors may be critical for the interaction.

The role of the hinge region of GR for its transactivation function and HEXIM1-mediated suppression

Next, to analyze the role of the hinge region of GR transactivation function and HEXIM1-mediated transcriptional suppression, wild-type and various mutant GR expression plasmids (See Fig. 2) were transfected with HEXIM1 expression plasmids and GRE-luciferase reporter plasmids in COS7 cells (Fig. 3A). As previously reported, wild-type GR-activated reporter gene expression was suppressed by HEXIM1, and the hinge region-deleted mutant GRdD1 was transcriptionally silent, however, GRdD2 was capable of inducing GRE-dependent transcription albeit weakly compared with wild-type GR (refs [12,15] and Fig. 3A). Of our surprise, DEX-induced transactivation of GRdD2 was also repressed by HEXIM1 (Fig. 3A). Since not only GRdD1 but also GRdD2 lacks interaction ability with HEXIM1, these results suggest that HEXIM1-mediated GR suppression is regulated mainly by direct interaction between GR and HEXIM1, but that, in the absence of that interaction, effect of sequestration of P-TEFb by HEXIM1 becomes evident. On the other hands, GRdD1 + MRD completely preserved HEXIM1-mediated repression as well as sufficient DEX-induced transactivation, as expected from the results in Fig. 2C. In contrast, GRdD1 + PPARγD and PPARγdD + GRD did not even activate GRE- or PPARRE-driven luciferase reporter gene in the presence of DEX or TGZ, respectively (Fig. 3A and B). Together, it is indicated that, although precise mechanisms remain unknown, the integrity of the receptor architecture involving the hinge region is important in transcriptional regulation by nuclear receptor, especially oxosteroid receptors including GR. In addition, the hinge region may be essential for GR-binding-mediated repression by HEXIM1.

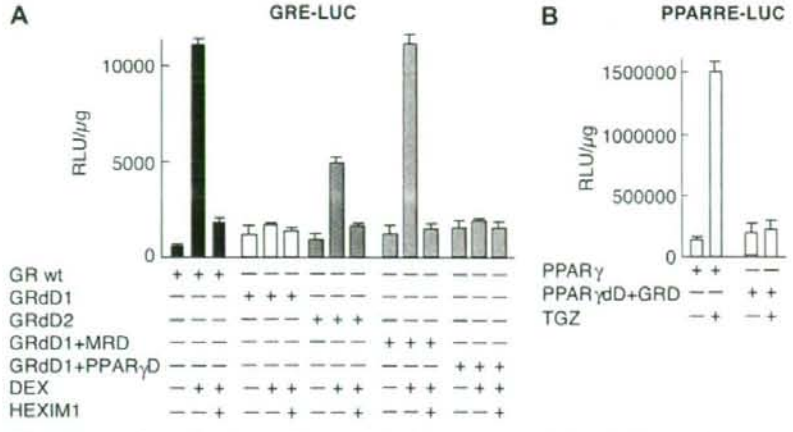

Fig. 3. The requirement of the hinge region of the nuclear receptors for their transactivation function and HEXIM1-mediated repression. (A,B) COS7 cells were cotransfected with 2 μg of reporter plasmids, pGRE-LUC (A) or pPPARRE-LUC (B), and 100 ng each of various receptor expression plasmids (also see Fig. 2C) with or without 500 ng of HEXIM1 expression plasmids as indicated, and further cultured with or without 100 nM DEX (A) or TGZ (B) for 24 h. The cell lysates were prepared for measurement of luciferase activities. All reporter gene experiments were performed in triplicate, results are expressed as relative light units (RLU) per microgram of protein in the extract, and means ± SD are shown.

HEXIM1 mutants lacking P-TEFb-binding ability suppressed GR-mediated but not PPARγ-mediated transactivation

To further analyze the molecular interplay between GR and HEXIM1, we used several HEXIM1 mutants that contain amino acid substitution in distinct portion of BR and differentially affect P-TEFb and GR activity as summarized in Fig. 4A. Those BR mutated HEXIM1 were classified according to the binding ability to P-TEFb, GR, and PPARγ, and tested in GRE- or PPARRE-driven reporter gene assays (Fig. 4B). HEXIM1 dBR + SV, which bound to neither P-TEFb, GR, nor PPARγ, did not affect reporter gene activity of PPARRE-LUC or GRE-LUC (Fig. 4B). Either HEXIM1 mutant, which could bind to GR (GR: + in Fig. 4A), suppressed ligand-dependent activation of GRE-driven reporter gene expression as well as wild-type HEXIM1, irrespective of P-TEFb-binding activity (Fig. 4B, *left panel*). In clear contrast, PPARγ-mediated activation of the reporter gene was repressed solely by wild-type HEXIM1 and 168–177A (P-TEFb: + in Fig. 4A) (Fig. 4B, *right panel*). In these experimental settings, HEXIM1 and its mutants did not affect protein expression of GR or PPARγ (data not shown). It, therefore, is indicated that direct interaction between GR and HEXIM1 plays a major role in HEXIM1-mediated suppression of GR, but that a certain category of the nuclear receptors such as PPARγ is negatively modulated by HEXIM1 solely via sequestration of P-TEFb.

Discussion

We previously revealed that HEXIM1 acts as a negative regulator of GR-mediated transcription, and that HEXIM1-binding to GR does not affect either ligand binding, nuclear translocation, or *in vitro* DNA-binding ability of GR [12]. Here we found that direct association of GR with HEXIM1 requires the hinge region of the receptor and HEXIM1 prefers oxosteroid receptors as an interacting partner among nuclear receptors. Indeed, amino acid sequence of the hinge region is least conserved across nuclear receptors, but the hinge region of GR is homologous only with those of the oxosteroid receptors (Fig. 2A). Although biological function of the very region remains largely unknown, several groups reported the biochemical interaction of the hinge region of GR with coregulatory proteins. For example, a eukaryotic cochaperone Bag1-M interacts with the hinge region of GR and negatively regulats GR action by inhibition of the ligand and DNA-binding activity of GR [6]. A nuclear receptor COUP-TFII also represses GR-induced transactivation by attracting a corepressor SMRT [7]. Moreover, it is demonstrated that the hinge region contains nuclear retention signal (NRS), overlapping with the NLS in GR [16]. In fact, the substitution of NRS dramatically weakens transactivational ability of GR [16]. We, therefore, cannot completely rule out such possibility that HEXIM1, via interacting with those coregulators or NRS, indirectly represses GR-mediated transcription. However, we previously showed that a certain fraction of HEXIM1 docks in the nucleus with GR [12], and the present study showed that the hinge region of GR is prerequisite for HEXIM1 binding at least *in vitro*. Moreover, our recent chromatin immunoprecipitation assays showed that HEXIM1 suppresses GR recruitment onto the target gene promoter (manuscript in preparation). We, therefore, favor such a model that at least part of HEXIM1 directly binds and sequesters GR to repress transcription initiation triggered by GR. Since it is generally considered that GR coactivators including TIF2 are recruited after GR binding to the promoter [4], this model may fit with our previous observation that overexpression of HEXIM1 decreases ligand-mediated GR-TIF2 association *in situ* [12]. In any case, it should be emphasized that the hinge region and its surrounding architecture may have multiple regulatory roles in GR-mediated signal transduction. The functional differences among GR, GRdD1, and GRdD2 strongly support this idea. Therefore, clarification of the molecular mechanism underlying this multimodal regulation of receptor function would be of importance to understand the integral role of the hinge region of GR.

Originally, it is estimated that majority of nuclear HEXIM1 forms complex with 7SK or Brd4, regulating expression of a large set of class II genes via intervening P-TEFb-mediated elongation reaction [10]. However, our present study rather highlights the distinct role of HEXIM1 independent from inhibition of elongation, gene-selective modulation of transcription. Recently, Montano et al. created mice carrying an insertional mutation in the HEXIM1 gene that disrupted its C-terminal region and found that the HEXIM1 C-terminal region is critical for cardiovascular development [13]. They indicated that HEXIM1 attenuates a repressive effect

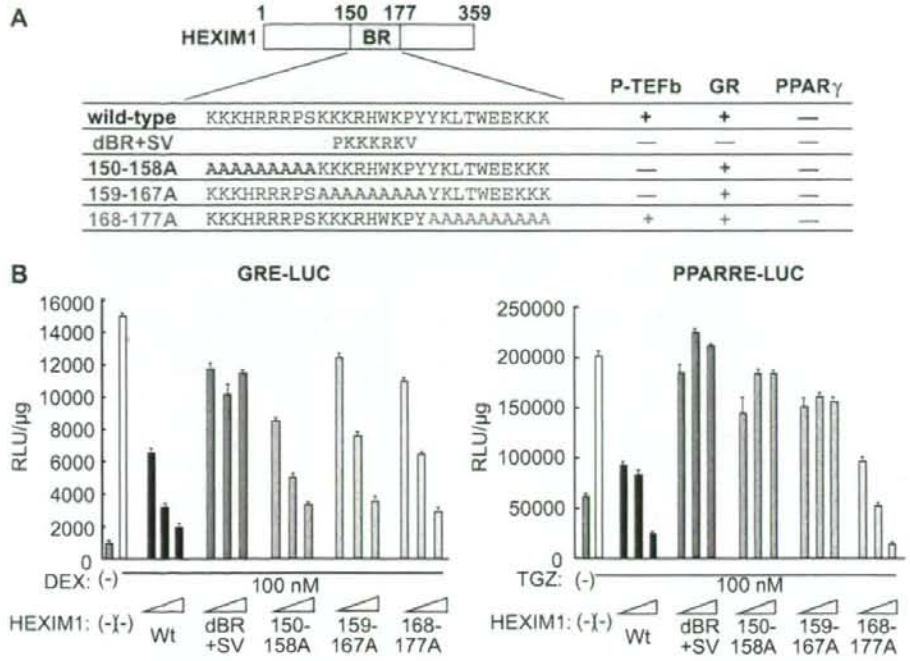

Fig. 4. HEXIM1 represses transactivation function of GR and PPARγ via functionally discrete mechanisms. (A) Primary structure of HEXIM1 (numbers depict amino acid positions), amino acid sequences of HEXIM1 mutants, and their interaction properties with P-TEFb, GR, and PPARγ are summarized. For testing P-TEFb binding, whole cell extracts of FLAG-tagged HEXIM1 or its mutants expressing HeLa cells were prepared and immunoprecipitated with anti-FLAG affinity resin, and CDK9 subunit of P-TEFb was detected using immunoblot. For testing GR and PPARγ binding to HEXIM1 and its BR mutants, various GST-fused HEXIM1-immobilized beads were incubated with *in vitro* translated [^{35}S]Met-labeled proteins, and bound receptors were analyzed on SDS–PAGE followed by fluorography. (B) COS7 cells were cotransfected with 2 μg each of pGRE-LUC (*left*) or pPPARRE-LUC (*right*) and 100 ng of expression plasmids for wild-type GR (*left*) or PPARγ (*right*), respectively, with or without increasing amounts (100, 500, and 1000 ng) of expression plasmids for HEXIM1 or its mutants as indicated. The cells were further cultured with or without 100 nM DEX (*left*) or TGZ (*right*) for 24 h and the cell lysates were prepared for measurement of luciferase activities. Experiments were performed in triplicate, results are expressed as relative light units (RLU) per microgram of protein in the extract, and means ± SD are shown.

of C/EBPα on vascular endothelial growth factor gene transcription. Note that C-terminal deletion of HEXIM1 does not affect P-TEFb inhibition [13]. Together with our study, it is strongly suggested that HEXIM1 may elicit modulation of gene expression not only via P-TEFb suppression but also via gene context-dependent mechanisms.

At this moment, many questions remain to be answered. It was reported that HEXIM1 represses transactivation function of ERα [11] which belongs to NR3A subfamily of the nuclear receptor superfamily [2]. They showed that HEXIM1 binds with ERα not via the hinge region but via the LBD [11]. Although the requirement of distinct domains for interaction with HEXIM1 between GR and ERα is interesting, we do not know how HEXIM1 can distinguish these two receptors classified in distinct subcategories of the nuclear receptor. This is also the case among oxosteroid receptors, since several members of this receptor group often are simultaneously expressed with fulfilling their own roles in the same tissue [17,18]. Similarly, it is also of particular importance to clarify how HEXIM1, using the central BR, differentially controls P-TEFb inhibition and GR suppression. Further studies, therefore, are clearly needed to address these issues. However, control of GR function *in situ* still remains to be a critical issue in medical fields [19]. Since HEXIM1 has a unique mode of modulation of GR function, HEXIM1 might be a pharmacological target for drug development to modulate GR function.

Acknowledgments

We thank the member of Morimoto laboratory for helpful suggestions. This work was supported by Grant-in-Aids for Science Research and Creative Scientific Research from the Ministry of Education, Culture, Sports, Science and Technology of Japan, and the Ministry of the Health, Labor, and Welfare of Japan to H. Tanaka. N. Shimizu is a postdoctoral fellow supported by the Japan Society for the Promotion of Science.

References

[1] R.M. Sapolsky, L.M. Romero, A.U. Munck, How do glucocorticoids influence stress responses? Integrating permissive, suppressive, stimulatory, and preparative actions, Endocr. Rev. 21 (2000) 55–89.
[2] Nuclear Receptors Nomenclature Committee, A unified nomenclature system for the nuclear receptor superfamily, Cell 97 (1999) 161–163.
[3] T. Rhen, J.A. Cidlowski, Antiinflammatory action of glucocorticoids-new mechanisms for old drugs, N. Engl. J. Med. 353 (2005) 1711–1723.
[4] M.G. Rosenfeld, V.V. Lunyak, C.K. Glass, Sensors and signals: a coactivator/corepressor/epigenetic code for integrating signal-dependent programs of transcriptional response, Genes Dev. 20 (2006) 1405–1428.
[5] R. Kumar, E.B. Thompson, Gene regulation by the glucocorticoid receptor: structure:function relationship, J. Steroid Biochem. Mol. Biol. 94 (2005) 383–394.
[6] M. Kullmann, J. Schneikert, J. Moll, S. Heck, M. Zeiner, U. Gehring, A.C. Cato, RAP46 is a negative regulator of glucocorticoid receptor action and hormone-induced apoptosis, J. Biol. Chem. 273 (1998) 14620–14625.

[7] M.U. De Martino, N. Bhattacharyya , S. Alesci, T. Ichijo, G.P. Chrousos, T. Kino, The glucocorticoid receptor and the orphan nuclear receptor chicken ovalbumin upstream promoter-transcription factor II interact with and mutually affect each other's transcriptional activities: implications for intermediary metabolism, Mol. Endocrinol. 18 (2004) 820–833.
[8] S. Malik, R.G. Roeder, Dynamic regulation of pol II transcription by the mammalian mediator complex, Trends Biochem. Sci. 30 (2005) 256–263.
[9] B.M. Peterlin, D.H. Price, Controlling the elongation phase of transcription with P-TEFb, Mol. Cell 23 (2006) 297–305.
[10] Q. Zhou, J.H. Yik, The Yin and Yang of P-TEFb regulation: implications for human immunodeficiency virus gene expression and global control of cell growth and differentiation, Microbiol. Mol. Biol. Rev. 70 (2006) 646–659.
[11] B.M. Wittmann, K. Fujinaga, H. Deng, N. Ogba, M.M. Montano, The breast cell growth inhibitor, estrogen down regulated gene 1, modulates a novel functional interaction between estrogen receptor alpha and transcriptional elongation factor cyclin T1, Oncogene 24 (2005) 5576–5588.
[12] N. Shimizu, R. Ouchida, N. Yoshikawa, T. Hisada, H. Watanabe, K. Okamoto, M. Kusuhara, H. Handa, C. Morimoto, H. Tanaka, HEXIM1 forms a transcriptionally abortive complex with glucocorticoid receptor without involving 7SK RNA and positive transcription elongation factor b, Proc. Natl. Acad. Sci. USA 102 (2005) 8555–8560.
[13] M.M. Montano, Y.Q. Doughman, H. Deng, L. Chaplin, J. Yang, N. Wang, Q. Zhou, N.L. Ward, M. Watanabe, Mutation of the HEXIM1 gene results in defects during heart and vascular development partly through downregulation of vascular endothelial growth factor , Circ. Res. (2007).
[14] N. Yoshikawa, K. Yamamoto, N. Shimizu, S. Yamada, C. Morimoto, H. Tanaka, The distinct agonistic properties of the phenylpyrazolosteroid cortivazol reveal interdomain communication within the glucocorticoid receptor, Mol. Endocrinol. 19 (2005) 1110–1124.
[15] S.M. Hollenberg, V. Giguere, P. Segui, R.M. Evans, Colocalization of DNA-binding and transcriptional activation functions in the human glucocorticoid receptor, Cell 49 (1987) 39–46.
[16] A. Carrigan, R.F. Walther, H.A. Salem, D. Wu, E. Atlas, Y.A. Lefebvre, R.J. Hache, An active nuclear retention signal in the glucocorticoid receptor functions as a strong inducer of transcriptional activation, J. Biol. Chem. 282 (2007) 10963–10971.
[17] E.R. de Kloet, R.H. Derijk, O.C. Meijer, Therapy insight: is there an imbalanced response of mineralocorticoid and glucocorticoid receptors in depression?, Nat Clin. Pract. Endocrinol. Metab. 3 (2007) 168–179.
[18] B.R. Walker, Glucocorticoids and cardiovascular disease, Eur. J. Endocrinol. 157 (2007) 545–559.
[19] F. Buttgereit, G.R. Burmester, B.J. Lipworth, Optimised glucocorticoid therapy: the sharpening of an old spear, Lancet 365 (2005) 801–803.

Biochemical and Biophysical Research Communications 369 (2008) 801–806

Contents lists available at ScienceDirect

Biochemical and Biophysical Research Communications

journal homepage: www.elsevier.com/locate/ybbrc

Common marmoset embryonic stem cell can differentiate into cardiomyocytes

Hao Chen [a,b], Fumiyuki Hattori [a,c], Mitsushige Murata [a,b], Weizhen Li [a], Shinsuke Yuasa [a], Takeshi Onizuka [a,b], Kenichiro Shimoji [a,b], Yohei Ohno [a,b], Erika Sasaki [d], Kensuke Kimura [a,b], Daihiko Hakuno [a,b], Motoaki Sano [a], Shinji Makino [a], Satoshi Ogawa [b], Keiichi Fukuda [a,*]

[a] Department of Regenerative Medicine and Advanced Cardiac Therapeutics, Keio University School of Medicine, 35 Shinanomachi, Shinjuku-ku, Tokyo 160-8582, Japan
[b] Division of Cardiology, Department of Medicine, Keio University School of Medicine, 35 Shinanomachi, Shinjuku-ku, Tokyo 160-8582, Japan
[c] Asubio Pharma Co., Ltd., 1-1-1 Wakayamadai, Shimamoto-cho, Mishima-gun, Osaka 618–8513, Japan
[d] Laboratory of Applied Developmental Biology, Marmoset Research Department, Central Institute for Experimental Animals, 1430 Nogawa, Miyamae-ku, Kawasaki, Kanagawa 216-0001, Japan

ARTICLE INFO

Article history:
Received 7 February 2008
Available online 10 March 2008

Keywords:
Embryonic stem cell
Common marmoset
Primate
Monkey
Cardiomyocytes
Differentiation
Characterization
Heart regeneration
Preclinical model

ABSTRACT

Common marmoset monkeys have recently attracted much attention as a primate research model, and are preferred to rhesus and cynomolgus monkeys due to their small bodies, easy handling and efficient breeding. We recently reported the establishment of common marmoset embryonic stem cell (CMESC) lines that could differentiate into three germ layers. Here, we report that our CMESC can also differentiate into cardiomyocytes and investigated their characteristics. After induction, *FOG-2* was expressed, followed by *GATA4* and *Tbx20*, then *Nkx2.5* and *Tbx5*. Spontaneous beating could be detected at days 12–15. Immunofluorescent staining and ultrastructural analyses revealed that they possessed characteristics typical of functional cardiomyocytes. They showed sinus node-like action potentials, and the beating rate was augmented by isoproterenol stimulation. The BrdU incorporation assay revealed that CMESC-derived cardiomyocytes retained a high proliferative potential for up to 24 weeks. We believe that CMESC-derived cardiomyocytes will advance preclinical studies in cardiovascular regenerative medicine.

© 2008 Elsevier Inc. All rights reserved.

Cardiomyocytes have been known to terminally differentiate and lose their ability to proliferate soon after birth [1]. Some researchers have reported the possible existence of adult cardiac stem or progenitor cells [2–4], but unfortunately these cells do not have sufficient proliferation ability for repairing the damaged heart [5]. Therefore, once the physical or functional loss of myocytes occurs due to myocardial infarction (MI) or myocarditis, a damaged heart cannot recover its structure and function. The characteristics of embryonic stem (ES) cells include clonal and unlimited expansion, as well as differentiation into various cell types including cardiomyocytes [6]. Thus, human ES cells would be an attractive cell source for regenerative heart therapy. However, before these can be applied clinically, the therapeutic efficacy and safety of ES cell-derived cardiomyocytes must be proven in preclinical experiments using a primate model system.

To date, rhesus and cynomolgus monkeys have been the most frequently used primate models in preclinical studies. Recently, the common marmoset monkey (*Callithrix jacchus*) has attracted a great deal of attention as a potential laboratory and preclinical experimental animal, because it has many advantages including a small body, a short gestation period (approximately 144 days), early sexual maturity (12–18 months), bears 4–6 progeny/year, is cost efficient and is easy to maintain. Recently, we reported the establishment of three CMESC lines, which have many similarities to human ES cells including morphology, surface antigens and cellular characteristics [7]. It is expected that common marmoset monkeys and CMESC-derived differentiated cells will provide a powerful preclinical model for studies in the field of regenerative medicine.

Rhesus and cynomolgus monkey ES cells have already been established [8,9], and these ES cells are able to differentiate into cardiomyocytes [10,11]. We have reported previously that CMESC lines can differentiate into neuron and glia, and induce formation of teratomas including cartilage, adipose tissue, skeletal muscle, a bronchus-like structure, keratinizing squamous epidermis, epidermis and CD31-positive vascular endothelial cells [7]. However, we were not able to induce cardiomyocyte differentiation from CMESC.

To utilize this system for preclinical studies into heart regeneration, we investigated conditions that were suitable for cardiomyocyte induction from CMESC. Here we report the successful

* Corresponding author. Address: Department of Regenerative Medicine and Advanced Cardiac Therapeutics, Keio University School of Medicine, 35 Shinanomachi, Shinjuku-ku, Tokyo 160-8582, Japan. Fax: +81 3 5363 3875.
E-mail address: kfukuda@sc.itc.keio.ac.jp (K. Fukuda).

0006-291X/$ - see front matter © 2008 Elsevier Inc. All rights reserved.
doi:10.1016/j.bbrc.2008.02.141

differentiation of CMESC into cardiomyocytes. The CMESC-derived cardiomyocytes were characterized in detail.

Materials and methods

Common marmoset ES cell culture and differentiation. The CMESC lines No. 20 and 40 were obtained from the Laboratory of Applied Developmental Biology, Marmoset Research Department, Central Institute for Experimental Animals [7]. CMESCs were cultured on 10 μg/mL mitomycin C-treated mouse embryonic fibroblast (MEF) feeder cells with CMESM (common marmoset ES cell medium) culture medium, which consisted of 80% Knockout Dulbecco's modified Eagle's medium (KO-DMEM; Invitrogen Co., 10829-018) supplemented with 20% Knockout Serum Replacement® (KSR; Invitrogen Co., 10828-028), 0.1 mM MEM Non-Essential Amino Acids Solution (Sigma–Aldrich Co., M7145), 2 mM L-Glutamine (Invitrogen Co., 25030-081), 0.1 mM β-Mercaptoethanol (2-ME; Sigma–Aldrich Co., M-7522) and 4 ng/mL basic fibroblast growth factor (bFGF; Wako Pure Chemical Industries Ltd., 064-04541). CMESCs were passaged every 5 or 6 days to maintain them in an undifferentiated state.

For differentiation, CMESC colonies of an appropriate size were chosen using a combination of 40-μm and 100-μm cell-strainers (Becton–Dickinson) that also facilitated the complete removal of feeder cells. Embryoid bodies (EBs) were formed by suspending and culturing colonies in Petri dishes during the first 10 days. To evaluate the incidence of beating EBs, EBs were distributed in non-adhesive 96-well culture plates (Sumitomo Bakelite Co., Ltd.) with approximately 1–2 EBs per well.

Reverse transcription-polymerase chain reaction (RT-PCR) analysis. Total RNA was prepared from EBs using ISOGEN (Nippon gene Co., Ltd., 317-02501), according to the manufacturer's instructions. Contaminating genomic DNA was degraded by RNase-Free DNase I (Ambion, Japan, #2222) at 37 °C for 30 min. Following phenol–chloroform extraction and ethanol precipitation, total RNA was reverse transcribed into cDNA using the Oligo-(dT)12-18 primer (Superscript II RT kit; Invitrogen Co., 18064-022) and then amplified by PCR using RED-Taq DNA polymerase (Sigma–Aldrich Co., D4309). The primer sequences and PCR conditions are listed online in Supplementary Table 1.

Immunofluorescent staining. EBs (6–8 weeks after differentiation) were fixed in 4% paraformaldehyde for 30 min at room temperature, cryoprotected with sucrose and cryosectioned into 7-μm sections. After pretreatment with ImmunoBlock® (Dainippon Sumitomo Pharma Co., Ltd., KN001), the sections were incubated at 4 °C overnight with the primary antibodies diluted in TBST (Tris-buffered saline with 0.1% Tween 20). The fluorescent dye-conjugated secondary antibodies were then applied to the sections for 30 min at 37 °C. The antibodies used in this study are listed online in Supplementary Table 2. The nuclei were stained with DAPI or ToPro-3 (Invitrogen Co.) and observed by conventional fluorescent microscopy (IX71; Olympus Co.) and confocal Laser microscopy (LSM510 META; Carl Zeiss Inc.), respectively.

Transmission electron microscopy (TEM). EBs were fixed in cold 2.5% glutaraldehyde with 2% paraformaldehyde in 0.1 mol/L cacodylate buffer (pH 7.4), post-fixed in 1% osmium tetroxide, dehydrated and embedded in Epon resin. Ultrathin sections were mounted on copper grids, stained with uranyl acetate and lead citrate, and examined by TEM (Philips).

Electrophysiology. The microscope was equipped with a recording chamber and a noise-free heating plate (Microwarm Plate; Kitazato Supply). A 10 mmol/L volume of HEPES was added to the culture medium to maintain the pH of the perfusate at 7.5–7.6. Standard glass microelectrodes that had a DC resistance of 25–35 MΩ when filled with pipette solution (2 mol/L KCl) were used. The electrodes were positioned using a motor-driven micromanipulator (EMM-3SV; Narishige) under optical control. Spontaneously beating cells were selected as targets, and the action potentials of the targeted cells were recorded. The recording pipette was connected to a patch-clamp amplifier (Axopatch 200B; Axon Instruments), and the signal was passed through a low-pass filter with a cut-off frequency of 2 kHz and digitized with an A/D converter with a sampling frequency of 10 kHz (Digidata 1440A; Axon Instruments). Signals were monitored, recorded as electronic files, and analyzed offline with pCLAMP 10 software (Axon Instruments).

BrdU incorporation assay. After three weeks of differentiation, the medium was changed and EBs were cultured in α-MEM supplemented with 10% FCS. Five to 36-week-old EBs were divided into two groups. EBs in Group 1 (intact EB) were cultured with 10 μmol/L of BrdU for 24 h in α-MEM supplemented with 10% FCS, then fixed with 4% paraformaldehyde. After treatment with 20% sucrose for 1 hour at RT, the fixed cells were cryosectioned. The sections were immersed in 2 N HCl with 0.5% Tween 20 solution for 20 min. Cardiomyocytes that had incorporated BrdU were detected using the BrdU Labeling and Detection Kit I (Roche Diagnostics Co., 11296736001) according to the manufacturer's instructions, except that the primary antibody for Nkx2.5 and the secondary antibody conjugated with Alexa-546 (Invitrogen Co.) were also used to identify cardiomyocytes. EBs in Group 2 (dispersed condition) were dispersed by 0.1% trypsin and 0.1% collagenase type III (Worthington Biochemical Co., #4182) in ADS buffer (116 mM NaCl, 20 mM HEPES, 12.5 mM NaH_2PO_4, 5.6 mM glucose, 5.4 mM KCl, and 0.8 mM $MgSO_4$, pH 7.35) with stirring. After 2 days of culture in α-MEM supplemented with 10% FCS, 10 μmol/L of BrdU was added and the dispersed EBs were cultured for a further 24 h at 37 °C in the same medium. Detection of BrdU-incorporated cardiomyocytes was performed as described above.

Results

Differentiation of CMESCs into spontaneously contracting cardiomyocytes

The two lines of CMESCs were cultured in medium containing KSR instead of animal-derived serum in order to maintain pluripotency (Fig. 1A, left). To stimulate the CMESCs to differentiate into cardiomyocytes, we adopted a conventional floating culture system and tested several combinations of medium (DMEM, KO-DMEM or α-MEM) and several lots of fetal calf serum (FCS) or KSR. We succeeded in stimulating CMESC line No. 20 to differentiate into contracting EBs, but failed to differentiate CMESC line No.40 under all conditions tested. CMESC line No. 20 could differentiate into EBs with contracting areas when a combination of three out of five lots of FCS (5–20% in use) and KO-DMEM or α-MEM were used. Strikingly, beating EBs could be obtained very efficiently by culturing the cells in KO-DMEM supplemented with 20% KSR, which was named dCMESM (common marmoset ES cell medium for cardiomyocyte differentiation). This had the same composition as the CMESM, but lacked bFGF. Confluent cultures of undifferentiated CMESCs were completely dissociated from the feeder cells and cultured in suspension to form EBs in dCMESM. In the floating culture system, CMESCs efficiently developed EBs and spontaneously beating cells (Supplementary Movie). An average of 10–20% of EBs began spontaneously contracting 12–15 days after differentiation. A maximum percentage (46 ± 13%) of contractile EBs was observed at approximately 18 days after differentiation, and was roughly sustained for two months.

Most contractile areas within EBs were located in the cell mass or the periphery of cystic structures. Contraction of CMESC-derived EBs was highly sensitive to temperature, a characteristic shared by human ES-derived EBs. EBs were cryosectioned 6–8 weeks after differentiation and immunofluorescent staining was performed. Typically Nkx2.5 and α-Actinin double-positive areas existed in the subsurface of EBs (Fig. 1A, center and right). In the cardiomyocyte-containing EBs, the Nkx2.5 and α-Actinin double-positive cells were approximately 30% of total cells.

Immunofluorescent staining and microstructure of CMESC-derived cardiomyocytes

Immunofluorescent staining was essential to determine the cardiomyocyte structure and the expression of cardiomyocyte-specific proteins. However, at the start of this study, the type of antibodies that would recognize common marmoset monkey cardiomyocytes was unknown. We therefore tested various antibodies that could detect cardiomyocyte-specific proteins in the CMESC-derived cardiomyocytes. Spontaneously beating EBs were dispersed and the CMESC-derived cardiomyocytes were cultured under adherent culture conditions. Immunofluorescent staining was then performed. Antibodies for the cardiac-specific transcription factors Nkx2.5 and GATA4 strongly labeled the nuclei of the CMESC-derived cardiomyocytes. Moreover, antibodies for α-Actinin, myosin heavy chain (MHC), myosin light chain (MLC) and Tropomyosin strongly labeled the typical myofilament structure of the cardiomyocytes. The antibody for the atrial natriuretic peptide (ANP) highlighted the secretary granules typical of cardiomyocytes surrounding the nucleus (Fig. 1B).

Microstructural analysis using TEM revealed typical myofilament structures, desmosomes and a number of mitochondria in CMESC-derived cardiomyocytes (Fig. 1C).

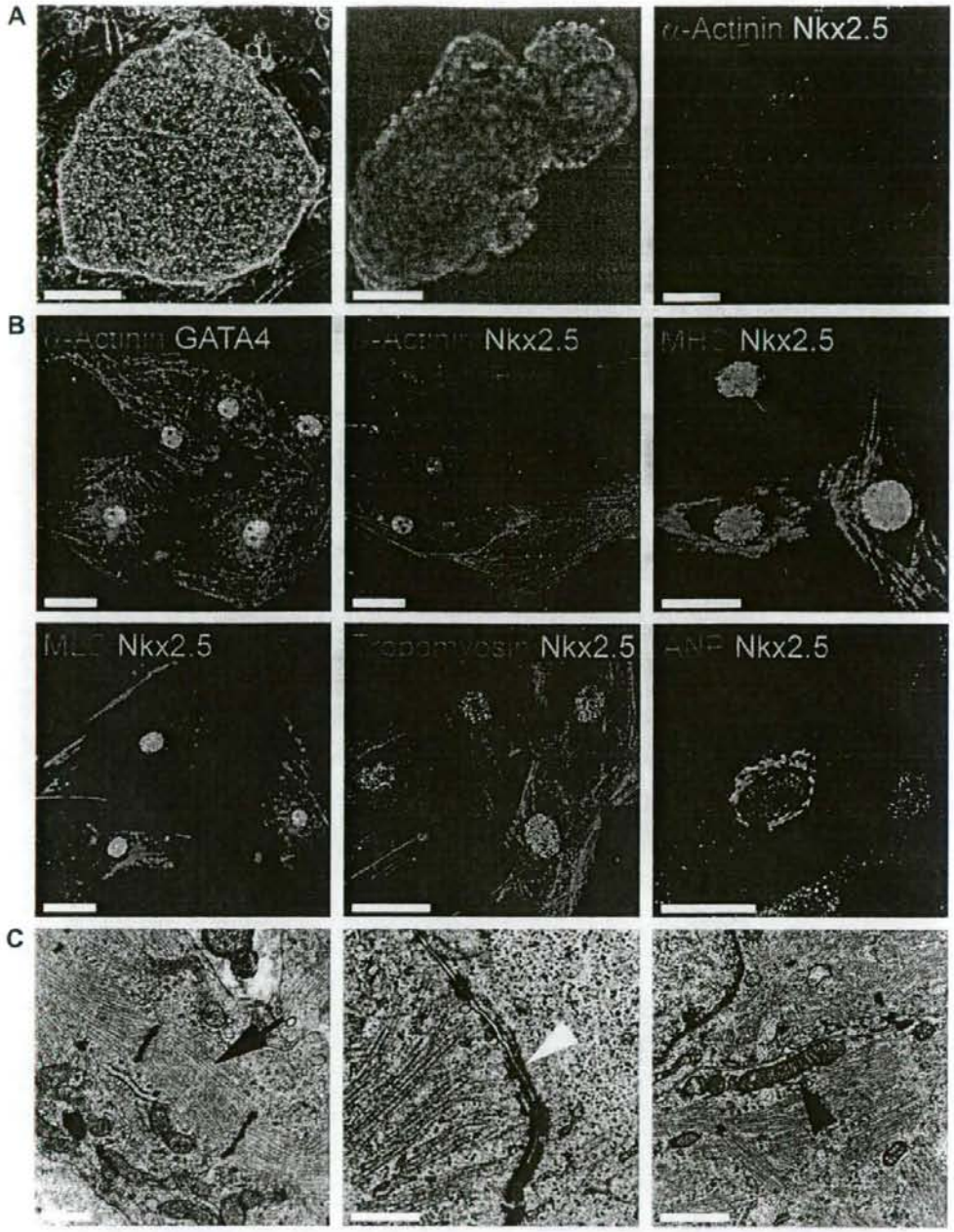

Fig. 1. Structural studies of CMESC-derived cardiomyocytes. (A) Phase contrast microscopy of the undifferentiated CMESC (left), and typical cardiomyocyte-containing non-cystic embryoid body (EB) (center). Immunofluorescent microscopy of cryosections of EBs using anti-α-Actinin and Nkx2.5 antibodies. (B) Double immunofluorescent staining for Nkx2.5 or GATA4 combined with α–Actinin, MHC, MLC, Tropomyosin or ANP. (C) Transmission electron microscopy of the CMESC-derived cardiomyocytes: striated muscle fiber (left, black arrow), desmosomal structure (middle, white arrow head) and mitochondria (right, black arrow head). Scale bars: (A) 100 μm; (B), 20 μm; (C) 0.5 μm.

Time course of marker gene expression during cardiomyocyte differentiation

To characterize the differentiation pathway of undifferentiated CMESC into cardiomyocytes, we performed semi-quantitative RT-PCR to analyze the expression of various marker genes associated with pluripotency, visceral endoderm, and early and late cardiomyogenesis. Some of the primers used have been described previously [7,10], and some were designed based on similar murine, *macaca fascicularis* and *homo sapiens* sequences (Supplementary Table 1). The pluripotency markers *Nanog* and octamer-binding transcription factor 3 (*Oct3/4*) were expressed at high levels in

undifferentiated ES cells. Expression levels of both markers gradually decreased upon differentiation and completely disappeared at day 15 post-differentiation (Fig. 2A). The early mesendoderm marker *Brachyury* was observed from day 3 post-differentiation, peaked at day 6 post-differentiation, but could not be detected at day 9 post-differentiation (Fig. 2B). The visceral endoderm marker alpha-fetoprotein (*AFP*) was observed from day 3 post-differentiation and peaked at day 9 post-differentiation, but could not be detected at day 15 post-differentiation (Fig. 2C). For the genes encoding cardiac-related transcription factors, the expression of the friend of GATA 2 (*FOG-2*) was first observed from day 3 post-differentiation, *GATA4* and the t-box 20 (*Tbx-20*) were from day 6 post-differentiation, *Tbx5* was from day 9 post-differentiation, and *Nkx2.5* was strongly observed at day 15 post-differentiation (Fig. 2D). For the cardiomyocyte-specific proteins, *ANP* and the MLC 2 atrial (*MLC2a*) were observed first from day 6 post-differentiation, *α-MHC* and *β-MHC* were from day 9 post-differentiation, the MLC 2 ventricular (*MLC2v*) was from day 12 post-differentiation (Fig. 2E).

Action potential recordings of CMESC-derived cardiomyocytes

We recorded the action potentials of CMESC-derived cardiomyocytes using glass microelectrodes. Eight-week-old contracting EBs were selected manually and dispersed into small clumps and single cells. The dispersed EBs were cultured to confluence for three days before analysis. The microelectrode was advanced to the intracellular cytoplasm and the voltage of the bulk solution and cytoplasm were measured. Rhythmic beating could be detected in the CMESC-derived cardiomyocytes. The action potential resembled a sinus node, indicating that the CMESC-derived cardiomyocytes had a relatively shallow resting membrane potential, slow diastolic depolarization and relatively long action potential duration (Fig. 3A). The administration of isoproterenol increased their beating rates (Fig. 3B). The basic cycle length (BCL), action potential duration (APD), d*V*/d*t*, action potential amplitude (APA) and maximum diastolic potential (MDP) were also recorded (Fig. 3C).

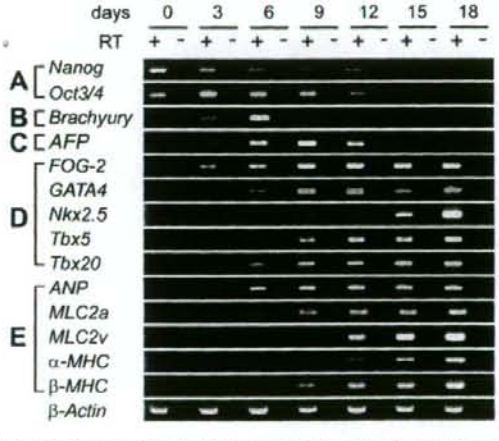

Fig. 2. RT-PCR analysis of the CMESC-derived EBs for various immature and cardiomyocyte-specific proteins. (A) Pluripotency-related genes: *Nanog* and *Oct3/4*; (B) Mesodermal marker gene: *Brachyury*; (C) Primitive endodermal marker gene: *AFP*; (D) cardiomyocyte-precursor and cardiomyocyte marker genes: *FOG-2*, *GATA4*, *Nkx2.5*, *Tbx5*, and *Tbx20*; (E) Cardiomyocyte-associated structural protein genes: *ANP*, *MLC2a*, *MLC2v*, *α-MHC*, *β-MHC*, and equal loading control β-actin. Reverse-transcription negative controls were also amplified and loaded in the lane next to the relevant sample. Abbreviations are listed in Supplementary Table 1.

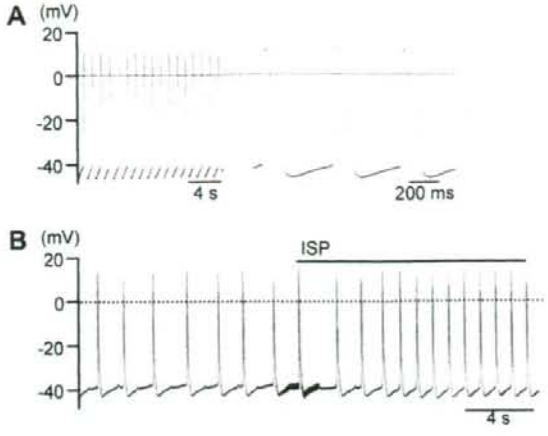

C

BCL (sec)	APD50 (msec)	APD90 (msec)
1.3~3.2	178.1±4.2	316.6±5.8

dV/dt max (V/s)	APA (mV)	MDP (mV)	n
5.6±1.0	68.4±2.5	-45.4±1.8	12

Fig. 3. Electrophysiology of CMESC-derived cardiomyocytes. (A) Representative action potentials of CMESC-derived cardiomyocytes showing spontaneous beating (left) and the relatively short duration time of the action potential (right). (B) Effect of isoproterenol (ISP) on the beating rate. (C) Statistical parameters obtained from 12 cardiomyocytes including beating cycle length (BCL), action potential duration (APD), d*V*/d*t* max, action potential amplitude (APA) and maximum diastolic potential (MDP).

Proliferative potential of CMESC-derived cardiomyocytes

Since the gestation period of the common marmoset is approximately seven times longer than that of the mouse, we hypothesized that CMESC-derived cardiomyocytes also retain their proliferative potential for a longer period of time and investigated this possibility. When EBs were dispersed into small clumps we observed a relatively long-term proliferation period and noticeable cell multiplication. From these findings, we expected that CMESC-derived cardiomyocytes might possess a higher proliferation ability than mouse-derived ES cells.

First, we performed BrdU incorporation assays on intact EBs at several time points after differentiation had occurred. The identification of DNA synthesizing cardiomyocytes was confirmed by co-immunofluorescent staining of Nkx2.5 and BrdU. At 6 weeks, intact EBs initially contained 33% BrdU-positive cardiomyocytes, but this decreased to less than 1% at 12 weeks (Fig. 4A and B). Next, the dispersed cells from EBs at several time points were applied to BrdU incorporation assays. Average 73% of cardiomyocytes were positive for BrdU at 5 weeks. This gradually decreased to 30% at 24 weeks, and 0% at 36 weeks (Fig. 4A and C). Most of the cardiomyocytes from freshly dispersed EBs 36 weeks after differentiation were rod-shaped (data not shown). These data indicated that common marmoset ES cell-derived cardiomyocytes retained their proliferation potential for an extended period of time.

Discussion

This is the first study to demonstrate that CMESC can differentiate into cardiomyocytes *in vitro*. We described their overall differentiation mechanism including time-courses for the expression of various genes during cardiogenesis, and characterized them in

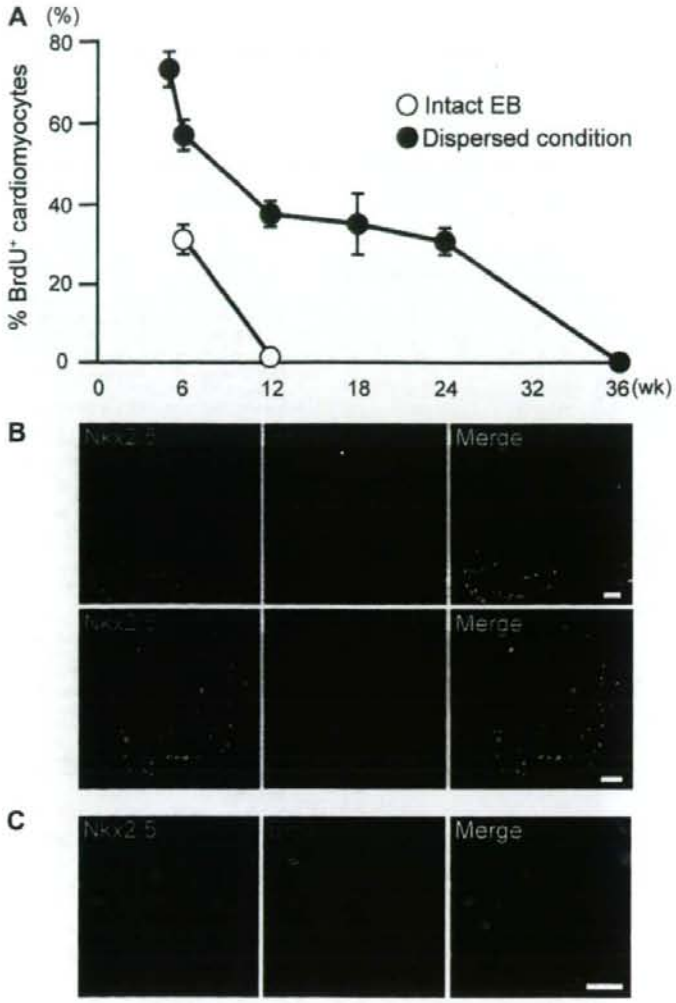

Fig. 4. Proliferation properties of CMESC-derived cardiomyocytes. (A) Time course BrdU incorporation assay in intact EB (open circle; $n = 3$) and dispersed condition (closed circle: $n = 3$) during weeks 5–36 post-differentiation. Cardiomyocytes were identified by immunofluorescent staining for Nkx2.5. The fractions of BrdU-positive cardiomyocytes were plotted. (B) Typical immunofluorescent staining patterns of Nkx2.5 (left), BrdU (middle) and merged images (right) in the intact EBs 6 weeks after differentiation (upper panel) and 12 weeks after differentiation (lower panel). (C) Typical immunodetection of Nkx2.5 (left), BrdU (middle) and merged images (right) in the dispersed condition 6 weeks after differentiation. Scale bars: (B) 100 μm; (C) 20 μm.

detail by immunofluorescent staining, ultrastructural analysis, electrophysiology and determining their growth properties.

Gene expression analyses during cardiogenesis in several species including mice [12], humans [13], and rhesus monkeys [10] are available. The present study enabled us to obtain gene expression data for the common marmoset monkey. A comparison of gene expression profiles between the species listed above highlights many similarities. The only major difference seems be in the timing of cardiomyocyte development: 8–14 days in humans; 12 days in the common marmoset; 8 days in the rhesus monkey; and 6 days in mice. Although minor differences in the expression timings of the *ANP*, *MLC-2a*, *MLC-2v* and *α-MHC* genes also exist during differentiation, we found that the timing of CMESCs was closest to human ES cells.

We found that the efficiency of cardiac differentiation was the same when obtained under non-serum conditions using KSR instead of FCS. These observations indicated that CMESCs, unlike human [14] or rhesus monkey [10] ES cells, do not require any serum-derived stimulating factors for mesendoderm induction and cardiogenesis, because KSR does not contain any cytokines or growth factors. On the other hand, the expression of various marker genes during cardiogenesis was very similar to that seen in human [14] and rhesus monkey [10] ES cells, suggesting that CMESCs have a similar cardiogenic differentiation system to human and rhesus monkey ES cells. CMESCs might be able to provide differentiation-inducing auto- and/or paracrine factors. Further mechanistic comparative studies between CMESCs and human and/or rhesus monkey ES cells will provide further insights into cardiogenic differentiation.

BrdU incorporation assay indicated that CMESC-derived cardiomyocytes were capable of long-term proliferation for extended periods of time. Importantly, CMESC-derived cardiomyocytes were still able to proliferate 24 weeks after differentiation, but the ability to proliferate ended at 36 weeks. Considering the gestation

period of the common marmoset, these findings had a reasonable explanation.

Much information about human ES cells and their application to heart regeneration therapy has accumulated [15,16]. Moreover, mouse and human inducible pluripotent stem cells (iPS cell) have also been established [17]. In order for heart regeneration therapy using regenerated cardiomyocytes to become a reality, preclinical studies using primate ES cell- or iPS cell-derived cardiomyocytes for transplantation are necessary. The common marmoset monkey is an ideal primate model for preclinical studies in the field of regenerative medicine. We believe that this report provides fundamental details about CMESC-derived cardiomyocytes that will aid their use as a primate heart cell-therapy model.

Appendix A. Supplementary data

Supplementary data associated with this article can be found, in the online version, at doi:10.1016/j.bbrc.2008.02.141.

References

[1] W.R. MacLellan, M.D. Schneider, Genetic dissection of cardiac growth control pathways, Annu. Rev. Physiol. 62 (2000) 289–319.
[2] B. Dawn, A.B. Stein, K. Urbanek, M. Rota, B. Whang, R. Rastaldo, D. Torella, X.L. Tang, A. Rezazadeh, J. Kajstura, A. Leri, G. Hunt, J. Varma, S.D. Prabhu, P. Anversa, R. Bolli, Cardiac stem cells delivered intravascularly traverse the vessel barrier, regenerate infarcted myocardium, and improve cardiac function, Proc. Natl. Acad. Sci. USA 102 (2005) 3766–3771.
[3] K.L. Laugwitz, A. Moretti, J. Lam, P. Gruber, Y. Chen, S. Woodard, L.Z. Lin, C.L. Cai, M.M. Lu, M. Reth, O. Platoshyn, J.X. Yuan, S. Evans, K.R. Chien, Postnatal isl1+ cardioblasts enter fully differentiated cardiomyocyte lineages, Nature 433 (2005) 647–653.
[4] H. Oh, S.B. Bradfute, T.D. Gallardo, T. Nakamura, V. Gaussin, Y. Mishina, J. Pocius, L.H. Michael, R.R. Behringer, D.J. Garry, M.L. Entman, M.D. Schneider, Cardiac progenitor cells from adult myocardium: homing, differentiation, and fusion after infarction, Proc. Natl. Acad. Sci. USA 100 (2003) 12313–12318.
[5] S. Lyngbaek, M. Schneider, J.L. Hansen, S.P. Sheikh, Cardiac regeneration by resident stem and progenitor cells in the adult heart, Basic Res. Cardiol. 102 (2007) 101–114.
[6] I. Kehat, D. Kenyagin-Karsenti, M. Snir, H. Segev, M. Amit, A. Gepstein, E. Livne, O. Binah, J. Itskovitz-Eldor, L. Gepstein, Human embryonic stem cells can differentiate into myocytes with structural and functional properties of cardiomyocytes, J. Clin. Invest. 108 (2001) 407–414.
[7] E. Sasaki, K. Hanazawa, R. Kurita, A. Akatsuka, T. Yoshizaki, H. Ishii, Y. Tanioka, Y. Ohnishi, H. Suemizu, A. Sugawara, N. Tamaoki, K. Izawa, Y. Nakazaki, H. Hamada, H. Suemori, S. Asano, N. Nakatsuji, H. Okano, K. Tani, Establishment of novel embryonic stem cell lines derived from the common marmoset (Callithrix jacchus), Stem Cells 23 (2005) 1304–1313.
[8] J.A. Thomson, J. Kalishman, T.G. Golos, M. Durning, C.P. Harris, R.A. Becker, J.P. Hearn, Isolation of a primate embryonic stem cell line, Proc. Natl. Acad. Sci. USA 92 (1995) 7844–7848.
[9] H. Suemori, T. Tada, R. Torii, Y. Hosoi, K. Kobayashi, H. Imahie, Y. Kondo, A. Iritani, N. Nakatsuji, Establishment of embryonic stem cell lines from cynomolgus monkey blastocysts produced by IVF or ICSI, Dev. Dyn. 222 (2001) 273–279.
[10] K. Schwanke, S. Wunderlich, M. Reppel, M.E. Winkler, M. Matzkies, S. Groos, J. Itskovitz-Eldor, A.R. Simon, J. Hescheler, A. Haverich, U. Martin, Generation and characterization of functional cardiomyocytes from rhesus monkey embryonic stem cells, Stem Cells 24 (2006) 1423–1432.
[11] M. Hosseinkhani, K. Hasegawa, K. Ono, T. Kawamura, T. Takaya, T. Morimoto, H. Wada, A. Shimatsu, S.G. Prat, H. Suemori, N. Nakatsuji, T. Kita, Trichostatin A induces myocardial differentiation of monkey ES cells, Biochem. Biophys. Res. Commun. 356 (2007) 386–391.
[12] K.R. Boheler, J. Czyz, D. Tweedie, H.T. Yang, S.V. Anisimov, A.M. Wobus, Differentiation of pluripotent embryonic stem cells into cardiomyocytes, Circ. Res. 91 (2002) 189–201.
[13] A. Beqqali, J. Kloots, D. Ward-van Oostwaard, C. Mummery, R. Passier, Genome-wide transcriptional profiling of human embryonic stem cells differentiating to cardiomyocytes, Stem Cells 24 (2006) 1956–1967.
[14] E. Bettiol, L. Sartiani, L. Chicha, K.H. Krause, E. Cerbai, M.E. Jaconi, Fetal bovine serum enables cardiac differentiation of human embryonic stem cells, Differentiation 75 (2007) 669–681.
[15] O. Caspi, I. Huber, I. Kehat, M. Habib, G. Arbel, A. Gepstein, L. Yankelson, D. Aronson, R. Beyar, L. Gepstein, Transplantation of human embryonic stem cell-derived cardiomyocytes improves myocardial performance in infarcted rat hearts, J. Am. Coll. Cardiol. 50 (2007) 1884–1893.
[16] M.A. Laflamme, K.Y. Chen, A.V. Naumova, V. Muskheli, J.A. Fugate, S.K. Dupras, H. Reinecke, C. Xu, M. Hassanipour, S. Police, C. O'Sullivan, L. Collins, Y. Chen, E. Minami, E.A. Gill, S. Ueno, C. Yuan, J. Gold, C.E. Murry, Cardiomyocytes derived from human embryonic stem cells in pro-survival factors enhance function of infarcted rat hearts, Nat. Biotechnol. 25 (2007) 1015–1024.
[17] K. Takahashi, S. Yamanaka, Induction of pluripotent stem cells from mouse embryonic and adult fibroblast cultures by defined factors, Cell 126 (2006) 663–676.

0888-8809/08/$15.00/0
Printed in U.S.A.

Molecular Endocrinology 22(12):2609–2623
Copyright © 2008 by The Endocrine Society
doi: 10.1210/me.2008-0101

Tissue- and Context-Dependent Modulation of Hormonal Sensitivity of Glucocorticoid-Responsive Genes by Hexamethylene Bisacetamide-Inducible Protein 1

Noriaki Shimizu,* Noritada Yoshikawa,* Tadashi Wada, Hiroshi Handa, Motoaki Sano, Keiichi Fukuda, Makoto Suematsu, Takashi Sawai, Chikao Morimoto, and Hirotoshi Tanaka

Division of Clinical Immunology (N.S., N.Y., C.M., H.T.), Advanced Clinical Research Center; Department of Rheumatology and Allergy (N.Y., C.M., H.T.), Research Hospital, Institute of Medical Science, University of Tokyo, Tokyo 108-8369, Japan; Department of Biological Information (T.W., H.H.), Graduate School of Bioscience and Biotechnology; Solutions Research Division (H.H.), Integrated Research Institute, Tokyo Institute of Technology, Yokohama 226-8501, Japan; Department of Regenerative Medicine and Advanced Cardiac Therapeutics (M.S., K.F.); Department of Biochemistry and Integrative Medical Biology (M.S.), Keio University School of Medicine, Tokyo 160-8582, Japan; and Department of Pathology I (T.S.), Iwate Medical University, Morioka 020-8505, Japan

Physiological and pharmacological processes mediated by glucocorticoids involve tissue- and context-specific regulation of glucocorticoid-responsive gene expression via glucocorticoid receptor (GR). However, the molecular mechanisms underlying such highly coordinated regulation of glucocorticoid actions remain to be studied. We here addressed this issue using *atp1a1* and *scnn1a*, both of which are up-regulated in response to corticosteroids in human embryonic kidney-derived 293 cells, but resistant in liver-derived HepG2 cells. Hexamethylene bisacetamide-inducible protein 1 (HEXIM1) represses gene expression via, at least, two distinct mechanisms, *i.e.* positive transcription elongation factor b sequestration and direct interaction with GR, and is relatively high in HepG2 cells compared with 293 cells. Given this, we focused on the role of HEXIM1 in transcriptional regulation of these GR target genes. In HepG2 cells, hormone resistance of *atp1a1* and *scnn1a* was diminished by either knockdown of HEXIM1 or overexpression of GR. Such a positive effect of exogenous expression of GR was counteracted by concomitant overexpression of HEXIM1, indicating the balance between GR and HEXIM1 modulates hormonal sensitivity of these genes. In support of this, the hormone-dependent recruitment of RNA polymerase II onto *atp1a1* promoter was in parallel with that of GR. Moreover, we revealed that not positive transcription elongation factor b-suppressing activity but direct interaction with GR of HEXIM1 plays a major role in suppression of promoter recruitment of the receptor and subsequent *atp1a1* and *scnn1a* gene activation. Collectively, we may conclude that HEXIM1 may participate in tissue-selective determination of glucocorticoid sensitivity via direct interaction with GR at least in certain gene sets including *atp1a1* and *scnn1a*. (*Molecular Endocrinology* 22: 2609–2623, 2008)

GLUCOCORTICOIDS ARE secreted from the adrenal glands under the strict control of the hypothalamic-pituitary-adrenal axis and maintain homeostasis through the regulation of electrolyte balance, glucose homeostasis, lipid and protein metabolism, and modulation of the immune, cardiovascular, and central nervous system (1–3). On the other hand, glucocorticoids have been widely and successfully used in treating a number of pathological states, *e.g.* inflammation and autoimmune disorders (4). It has been demonstrated that such physiological and pharmacological processes mediated by glucocorticoids involve tissue-specific regulation of glucocorticoid-responsive gene expression (3). Moreover, glucocorticoid sensitivity of every single gene has been shown to differ among cells, tissues, and individuals, and even fluctuates not only in pathological states, but also during normal physiological processes, including development and the cell cycle (4, 5). Albeit its importance, the molecular mechanisms underlying highly coordinated tissue- and context-dependent regulation of expression of glucocorticoid-target genes remain to be studied.

First Published Online September 18, 2008

* N.S. and N.Y. contributed equally to this work, and both should be considered as first authors.

Abbreviations: AhR, Arylhydrocarbon receptor; BR, basic region; CDK9, cyclin-dependent kinase 9; ChIP, chromatin immunoprecipitation; CycT1, cyclin T1; DEX, dexamethasone; GR, glucocorticoid receptor; GRE, glucocorticoid response element; HA, hemagglutinin; HSF, heat shock factor; 3MC, 3-methylcholantrene; MOI, multiplicity of infection; PPAR, peroxisome proliferator-activated receptor; PPARRE, PPAR response element; qRT-PCR, quantitative real-time RT-PCR; P-TEFb, positive transcription elongation factor b; RNAPII, RNA polymerase II; siRNA, small interfering RNA; SDS, sodium dodecyl sulfate; snRNA, small nuclear RNA; SR, siRNA-resistant; STAT3, signal transducer and activator of transcription 3; SV, simian virus; TGZ, troglitazone; TSA, trichostatin A.

***Molecular Endocrinology* is published monthly by The Endocrine Society (http://www.endo-society.org), the foremost professional society serving the endocrine community.**

Downloaded from mend.endojournals.org at Keio Univ Igakubu Library on March 27, 2009

atp1a1 is expressed in all mammalian cells, and its product Na^+, K^+-ATPase α1 plays essential roles in regulating ionic intracellular milieu, the process that is needed for the regulation of metabolism, proliferation, differentiation, and cell volume (6). In addition, in kidney, Na^+, K^+-ATPase α1 also plays a central role in the fine control of systemic electrolyte balance through hormone-regulated sodium reabsorption, in functional cooperation with amiloride-sensitive Na^+ channel, which is encoded by *scnn1a* (7–9). *atp1a1*, as well as *scnn1a*, is up-regulated in response to corticosteroids in kidney (7). On the other hand, particularly in liver, expression of either *atp1a1* or *scnn1a* is not influenced by glucocorticoids, indicating that these genes are resistant to glucocorticoids, not in kidney but in liver. Interestingly, their hormone resistance seems to be corticosteroid signal selective, because other extracellular stimuli, such as thyroid hormones (10) and low external potassium ion (11), were shown to modulate mRNA expression of *atp1a1* even in liver.

Glucocorticoids elicit their hormone actions via a signal pathway involving ubiquitously expressed glucocorticoid receptor (GR), a prototypic member of the nuclear receptor superfamily, which acts as a ligand-dependent transcription factor (12). It is generally believed that, upon binding glucocorticoids, GR translocates into the nucleus and binds the glucocorticoid response element (GRE) on the target gene promoters. Binding of liganded receptors with target DNA is followed by recruitment of mediators and coactivators to the proximity of the target DNA, resulting in RNA polymerase II (RNAPII) recruitment and activation of transcription (4, 13–19). The recent advent of DNA microarray technology has revealed that there are only modest overlaps in glucocorticoid-regulated gene sets among different cell types. In fact, considerable numbers of genes are responsive to glucocorticoids in certain tissues but resistant in others (20–23). Already several mechanisms have been postulated for tissue-specific regulation of glucocorticoid actions including different metabolisms of ligands (24), tissue-specific cofactor availability (25), and GR subtype distribution (26).

Hexamethylene bisacetamide-inducible protein 1 (HEXIM1) was originally identified as a nuclear protein, expression of which was induced when human vascular smooth muscle cells were treated with hexamethylene bisacetamide, an inhibitor of cell proliferation (27). HEXIM1 has been shown to regulate mRNA expression via, at least, two distinct mechanisms, *i.e.* positive transcription elongation factor b (P-TEFb)-dependent (28, 29) and P-TEFb-independent mechanisms (30). P-TEFb, typically composed of cyclin-dependent kinase 9 (CDK9) and its regulatory partner cyclin T1 (CycT1), phosphorylates the C-terminal domain of RNAPII, thereby stimulating transcription elongation (31–33). P-TEFb recruitment has been reported in diverse class II promoters in association with a certain class of transcription factors, including HIV-1 Tat (34), nuclear factor-κB (35), signal transducer and activator of transcription 3 (STAT3) (36), heat shock factor (HSF) (37), and arylhydrocarbon receptor (AhR) (38). HEXIM1 exerts its inhibitory effect on P-TEFb *in vivo* and *in vitro* in a 7SK small nuclear RNA (snRNA)-dependent fashion (28, 29). Upon binding with HEXIM1 and 7SK snRNA, P-TEFb looses its kinase activity, resulting in suppression of transcription elongation (39, 40). On the other hand, several reports described P-TEFb-independent mechanisms of gene regulation by HEXIM1 (30, 41–47). Among others, we demonstrated that HEXIM1 directly interacts with GR and modulates glucocorticoid-responsive gene expression (30). Moreover, we recently showed that GR, via its hinge region, interacts with central basic amino acid-rich region of HEXIM1 (48). At this moment, however, it remains unknown how genes can differentially use these distinct functions of HEXIM1: inhibitory effects on P-TEFb-dependent elongation and GR-mediated transactivation.

In the present study, we showed that mRNA expression of *atp1a1* and *scnn1a* was up-regulated by treatment with glucocorticoids in human embryonic kidney-derived 293 cells, but not in human liver cancer-derived HepG2 cells. Knockdown of endogenous HEXIM1 in HepG2 cells canceled glucocorticoid resistance of *atp1a1* and *scnn1a* mRNA expression. By creating a system that enables differential analysis of the above-mentioned distinct HEXIM1 functions, we revealed that not P-TEFb-suppressing activity but direct interaction with GR plays a major role in suppression of *atp1a1* activation by attenuating promoter recruitment of the receptor and RNAPII. We may conclude, therefore, that HEXIM1 may participate in tissue- and gene-selective determination of glucocorticoid sensitivity via direct interaction with GR, at least in a certain gene set that includes *atp1a1* and *scnn1a*.

RESULTS

Dexamethasone (DEX)-Resistance of *atp1a1* and *scnn1a* Not in 293 Cells but in HepG2 Cells

Expression of *atp1a1* and *scnn1a* is shown to be up-regulated by glucocorticoids, as well as aldosterone, in kidney and kidney-derived 293 cells. On the other hand, in liver, their mRNA expression is induced by various intra- or extracellular stimuli except for glucocorticoids (see "Introduction"). That is, *atp1a1* and *scnn1a* appear to be resistant rather selectively against glucocorticoid-GR system particularly in liver. To address the molecular mechanism of such tissue-dependent hormone resistance in gene regulation, we studied HepG2 cells as a model in comparison with 293 cells. When we analyzed their mRNA expression levels using quantitative real-time RT-PCR (qRT-PCR), 6 h treatment of 293 cells with 100 nM DEX induced *atp1a1* and *scnn1a* mRNA expression by 1.9-fold and

Downloaded from mend.endojournals.org at Keio Univ Igakubu Library on March 27, 2009

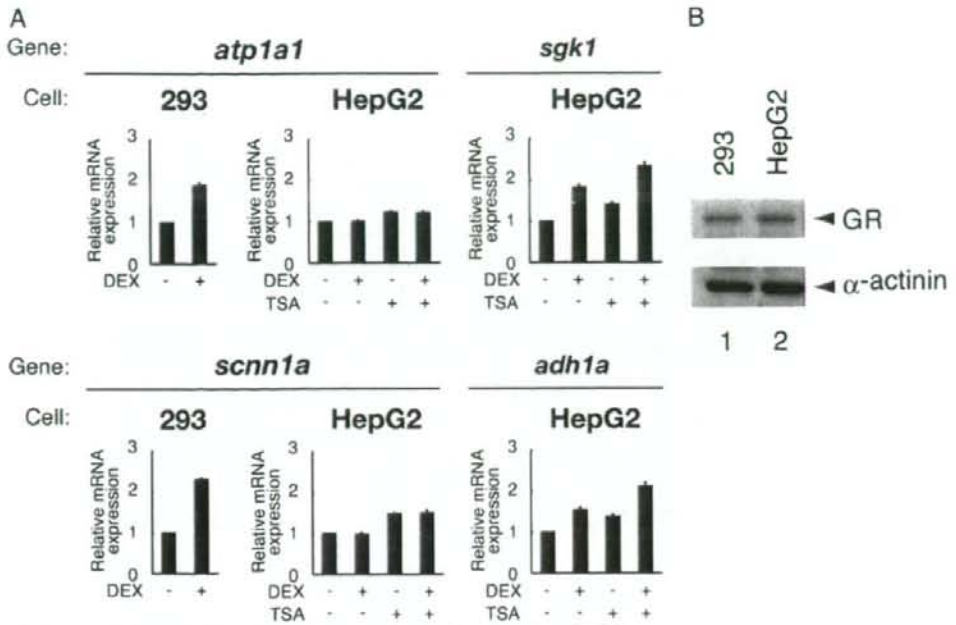

Fig. 1. DEX Resistance of *atp1a1* and *scnn1a* Not in 293 Cells but in HepG2 Cells

A, 293 cells and HepG2 cells were cultured in phenol red-free Opti-MEM I for 24 h and treated with or without 100 nM DEX for 6 h in the presence or absence of 100 nM TSA, as indicated. Total RNA was prepared and endogenous mRNA for Na^+, K^+-ATPase α1 (*atp1a1*), amiloride-sensitive Na^+ channel 1α (*scnn1a*), serum and glucocorticoid-regulated kinase 1 (*sgk1*), alcohol dehydrogenase 1A (*adh1a*), and glyceraldehyde-3-phosphate dehydrogenase (*gapdh*) was measured with qRT-PCR. Samples were normalized to *gapdh* mRNA levels, and relative expression levels to vehicle-treated samples are presented as relative mRNA expression. *Error bars* represent SD values of at least three independent experiments. B, Cell lysates from 293 cells and HepG2 cells were subjected to Western blot analysis using indicated antibodies.

2.3-fold, respectively (Fig. 1A). In contrast, mRNA expression of neither *atp1a1* nor *scnn1a* was induced in the presence of 100 nM DEX in HepG2 cells (Fig. 1A). Our previous DNA microarray analysis also supported this notion (data not shown). Note that GR is comparably expressed in HepG2 cells and 293 cells (Fig. 1B), and that mRNA expression of *sgk1* and *adh1a*, both of which are known to be glucocorticoid target genes as well (20–23), are induced by 1.8-fold and 1.6-fold, respectively, after DEX treatment in HepG2 cells (Fig. 1A). It is indicated, therefore, that, despite the presence of functional GR, mRNA expression of a particular set of genes, *i.e. atp1a1* and *scnn1a*, shows a cell- or tissue-specific resistance to glucocorticoids. Treatment with a histone deacetylase inhibitor trichostatin A (TSA) increased both basal and induced mRNA levels of *sgk1* and *adh1a*, but, in the case of *atp1a1* and *scnn1a*, only basal mRNA levels were increased without restoration of responsiveness to DEX (Fig. 1A). Glucocorticoid insensitivity of *atp1a1* and *scnn1a* in HepG2 cells, thus, does not appear to be related to histone acetylation-dependent mechanisms.

Cell Type Difference in Hormone-Dependent GR Recruitment onto GRE in *atp1a1* Promoter

In GR-dependent transactivation, binding of liganded receptors onto target DNA is generally believed to be an essential trigger for transcription initiation and elongation (12–15). We, therefore, tested *in vivo* occupancy of *atp1a1* promoter by endogenous GR in comparison with *sgk1* promoter using chromatin immunoprecipitation (ChIP) assay, because both promoters are known to contain GRE (Fig. 2A) (49, 50). In HepG2 cells, when *sgk1* promoter was tested, GR was recruited onto the promoter in a time- and hormone-dependent manner. In contrast, *atp1a1* promoter did not recruit GR even in the presence of DEX (Fig. 2A). Next, to examine the relationship between GR recruitment and ongoing transcription, we compared GR binding and RNAPII binding on *atp1a1* promoter after DEX treatment. RNAPII binding, as well as that of GR, was not increased after DEX treatment in HepG2 cells. In clear contrast, RNAPII binding was enhanced after DEX treatment in concert with increase of GR binding in 293 cells (Fig. 2B). These results indicate that glucocorticoid

Downloaded from mend.endojournals.org at Keio Univ Igakubu Library on March 27, 2009

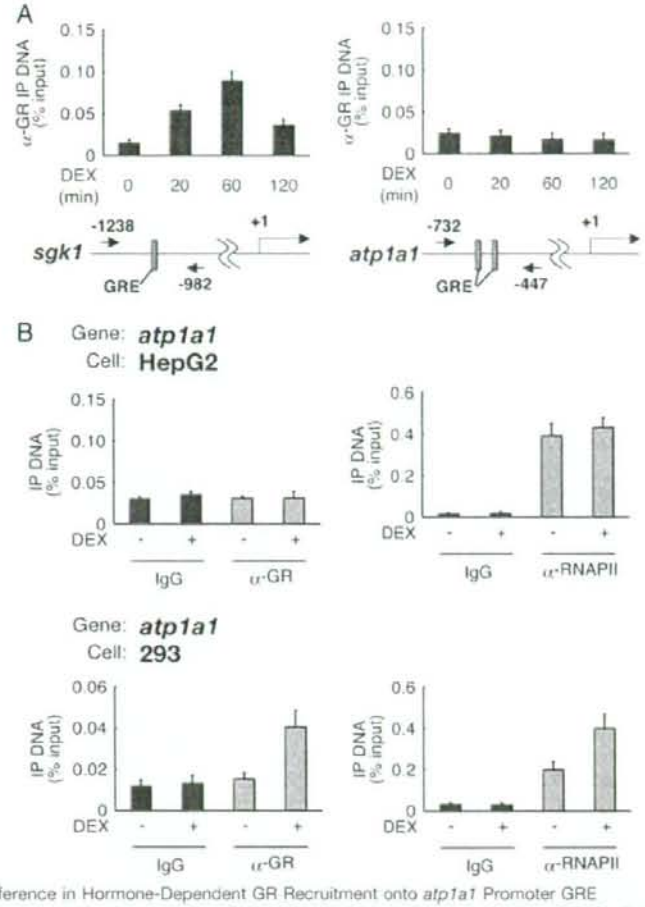

Fig. 2. Cell Type Difference in Hormone-Dependent GR Recruitment onto *atp1a1* Promoter GRE

A, HepG2 cells were cultured in phenol red-free Opti-MEM I for 24 h and treated with 1 μM DEX for the indicated time periods. ChIP assays were performed with anti-GR polyclonal antibodies, and recovered GRE-containing DNA fragments were measured with qRT-PCR. GREs in *sgk1* and *atp1a1* 5′-flanking regions are indicated as *gray boxes*. The positions of the primers are shown as *numbered arrows*. Values are expressed as percentage of immunoprecipitated DNA to input. *Error bars* represent SD values of at least three independent experiments. B, HepG2 cells and 293 cells were cultured as described in panel A and treated with 1 μM DEX for 60 min. ChIP assays were performed with the indicated antibodies and primer sets as described in *Materials and Methods*. IP, Immunoprecipitation.

resistance of *atp1a1* promoter may be due to cell type-dependent deficiency of GR recruitment despite the presence of the receptor.

Endogenous HEXIM1 Negatively Modulates Glucocorticoid-Mediated Transcriptional Activation

It was previously described that HEXIM1 mRNA is ubiquitously expressed but its expression levels are variable among human tissues (27). Protein expression levels of endogenous HEXIM1 also show a great diversity among tissues in mice; HEXIM1 expression levels appeared to be low in kidney compared with those in liver, brain, lung, spleen, and heart (Fig. 3A). These tissue-dependent differences of HEXIM1 expression levels were also observed in human tissue-derived cell lines, *i.e.* HepG2 cells abundantly express HEXIM1 compared with 293 cells (Fig. 3A). Together with the fact that certain GR target genes, *e.g. atp1a1* and *scnn1a*, are resistant to hormone treatment in HEXIM1-rich HepG2 cells, we hypothesized that HEXIM1 may participate in cell type-dependent hormone resistance at the level of transcriptional regulation of these genes.

Given this, we then addressed whether endogenous HEXIM1 contributes to glucocorticoid insensitivity of

Downloaded from mend.endojournals.org at Keio Univ Igakubu Library on March 27, 2009

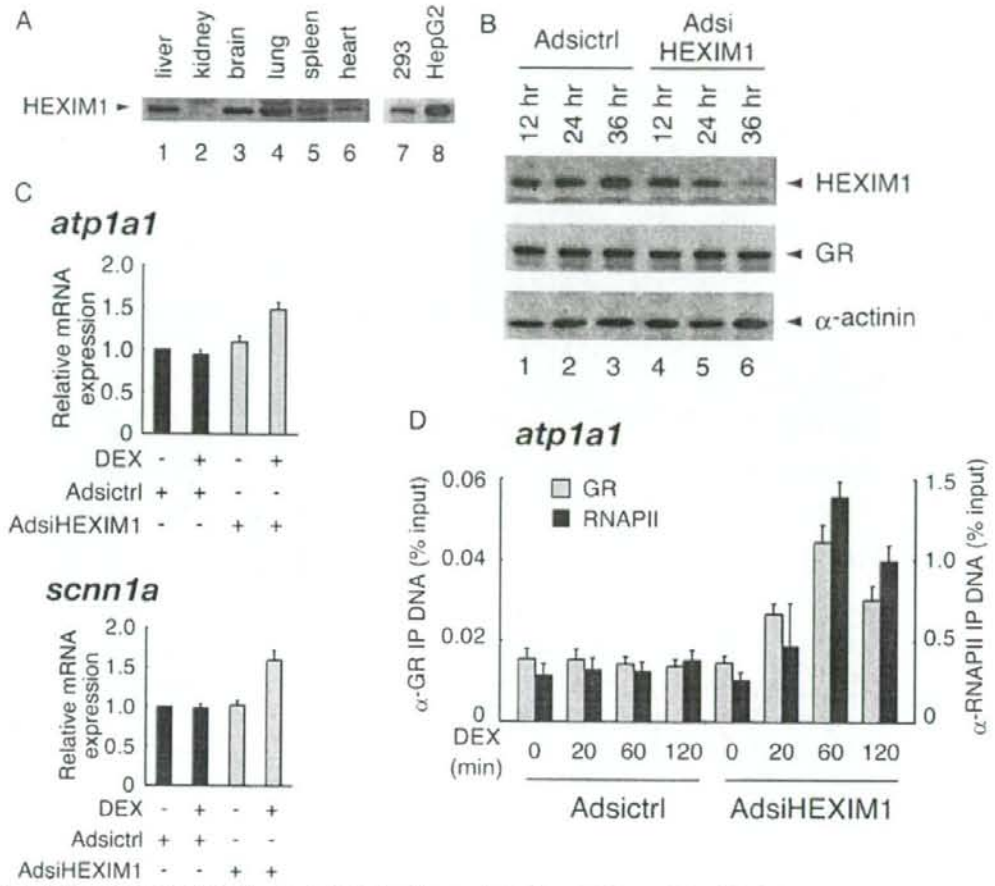

Fig. 3. Endogenous HEXIM1 Negatively Modulates Glucocorticoid-Mediated Transcriptional Activation

A, Cell lysates from various tissues from adult mice were subjected to Western blot analysis using indicated antibodies. B, HepG2 cells were infected with Adsictrl or AdsiHEXIM1 in phenol red-free Opti-MEM I at MOI of 100 for indicated time periods. Whole-cell extracts were prepared, and protein expression levels of endogenous HEXIM1, GR, and α-actinin were assessed in Western blotting. C, HepG2 cells were infected with the recombinant adenoviruses for 36 h as described in panel B and stimulated with 100 nM DEX for 6 h. Total RNA was prepared and mRNA for *atp1a1*, *scnn1a*, and *gapdh* was measured with qRT-PCR. Samples were normalized to *gapdh*, and relative expression levels to vehicle-treated samples are presented as relative mRNA expression. *Error bars* represent SD values of at least three independent experiments. D, HepG2 cells were infected with the recombinant adenoviruses for 36 h as described in panel B and stimulated with 1 μM DEX for indicated time periods. ChIP assays were performed with the indicated antibodies as described in *Materials and Methods*. IP, Immunoprecipitation.

atp1a1 and *scnn1a* in HepG2 cells. For that purpose, we constructed the recombinant adenoviruses expressing small interfering RNA (siRNA) against HEXIM1 named Adsi-HEXIM1, and unrelated siRNA named Adsictrl, as described in *Materials and Methods*. Figure 3B shows that infection of AdsiHEXIM1 diminished endogenous HEXIM1 protein expression down to less than 10% of the control without significant alteration of GR protein expression level. Again, mRNA expression of *atp1a1* and *scnn1a* was not significantly induced in the presence of 100 nM DEX in Adsictrl-infected HepG2 cells (Fig. 3C). Infection of AdsiHEXIM1 had little effect on basal levels of but significant effect on DEX-inducibility of *atp1a1* and *scnn1a* (Fig. 3C). Using *atp1a1* as a model, we then studied the influence of knockdown of endogenous HEXIM1 on hormone-dependent GR recruitment onto *atp1a1* promoter in ChIP analysis. As shown in Fig. 3D, GR was recruited in a time-dependent manner onto the promoter after DEX treatment in AdsiHEXIM1-infected cells. Moreover, RNAPII was also incorporated to the promoter in parallel with GR recruitment (Fig.

Downloaded from mend.endojournals.org at Keio Univ Igakubu Library on March 27, 2009